Neuroprotective micro RNAs as a potential therapeutic for HIV-associated neurocognitive disorders

by

Naveen Suresh Babu

B. Tech., Anna University, 2019

Submitted to the Graduate Faculty of the

Department of Infectious Diseases and Microbiology

Graduate School of Public Health partial fulfilment

of the requirements for the degree of

Master of Science

University of Pittsburgh

2020

UNIVERSITY OF PITTSBURGH

GRADUATE SCHOOL OF PUBLIC HEALTH

This thesis was presented

by

Naveen Suresh Babu

It was defended on

April 12, 2021

and approved by

Committee Chair and Thesis Advisor
Dr. Velpandi Ayyavoo, Professor and Assistant Chair
Dept. of Infectious Diseases and Microbiology
Graduate School of Public Health

Dr. Jeremy Martinson, Assistant Professor
Dept. of Infectious Diseases and Microbiology
Graduate School of Public Health

Dr. Yuanpu Peter Di, Associate Professor
Dept. of Environmental and Occupational Health
Graduate School of Public Health

Neuroprotective micro RNAs as a potential therapeutic for HIV-associated neurocognitive disorders

Naveen Suresh Babu, MS

University of Pittsburgh, 2021

ABSTRACT

Around 75 million people have been infected with the Human Immunodeficiency Virus-1 (HIV-1) since the inception of the epidemic, and it is estimated that nearly 38 million people are now living with the virus. As many as 50% of these individuals develop HIV-associated neurocognitive disorders (HAND) despite being on antiretroviral therapy. This process involves progressive loss of synaptic plasticity and dendritic morphology leading to motor problems, loss of memory, speech impairment and overall reduced quality of life. The constellation of symptoms associated with HAND seems to arise from virus-associated immune activation involving the microglia and macrophages in the CNS niche. Previous findings from our laboratory have indicated the differential expression of certain miRNAs in the PBMCs HIV+ HAND+ patients. Furthermore, preliminary data have suggested that these endogenous micro RNAs might have therapeutic potential in treating HAND. Based on these observations, we hypothesized that overexpression of these miRNAs in microglia might abate HIV-mediated inflammation and subsequent damage due to it. Results indicate that overexpression of miR-20a and miR-106b through lentiviral transduction reduced pro-inflammatory cytokine expression (especially TNF-α) during HIV-1 infection. Furthermore, miR-106b appears to hinder active HIV-1 replication suggesting a possible antiviral activity of this particular miRNA candidate. If successful, these miRNAs would eventually lead to a new class of antiretroviral drugs to curb infection, inflammation, and neurodegeneration due to HIV-1.

TABLE OF CONTENTS

LIST OF FIGURES

LIST OF TABLES

PREFACE

Firstly, I would like to thank my mentor, Dr. Velpandi Ayyavoo for providing me with the Fogarty scholarship and easing the financial burden of graduate school. Her tenacity, candidness, and passion for doing great science have imbibed me with great skills and responsibilities for my scientific career moving forward. As I leave her lab and move on to the next phase of my life, I look back at moments where I failed, moments where I learnt and moments where I persevered. These are the moments when Dr. Ayyavoo pushed me to give my best. Thank you for that!

Secondly, I would like to extend my thanks to Ms. Shrutika Jadhav for being a home away from home. We started as acquaintances but now she is an elder sister to me. You never gave up on me even when I did not want to move forward with life and science. Thank you for being my rock and my emotional support these past two years. I could not have done it without you.

I would like to take this opportunity to thank Dr. Robbie Mailliard, Dr. Jeremy Martinson, and Dr. Joshua Mattila for their extreme support and trust in my talent and skill. All of you had my back when times were tough, and I am indebted for it! I would also like to thank Dr. Peter Di for being my committee member and for extending invaluable advice to push my project forward. I also sincerely thank Ms. Jennifer Bowling, Ms. Vaishali Muralidaran, Ms. Rutuja Deshmukh and all other IDM folks for making me feel comfortable and making me feel belonged.

Last, but not the least, I extend my sincere gratitude to my undergraduate mentor Dr. P Gautam and my parents back home. It is their unwavering belief in my abilities that gave me the courage to uproot myself out of nativity to a foreign land for my career. For that, I owe my entire career to all of you moving forward!

1.0 INTRODUCTION

Since the beginning of the HIV-1 pandemic, approximately 75 million people have been infected with HIV-1. According to a recent UNAIDS report, there were 1.7 million new HIV-1 infections at the end of 2018 (1). As the epidemic progressed, both the adjusted mortality rate and incidence rate of new HIV-1 infections have greatly reduced (2). Novel scientific research and increased awareness about HIV/AIDS has led to this significant decrease in mortality. With the introduction of antiretroviral therapy (ART), a 28% increase in survival rates was observed between 2006 and 2012 (3). Antiretroviral therapy has now become a major determinant in the management of HIV-1 infections and has led to the near-complete absence of viral load in the patients' plasma. It was also found to lower the risk of sexual, blood borne and vertical modes of transmission by up to 90% (4). Additionally, the advent of pre-exposure prophylaxis for high-risk individuals as a preventive strategy has reduced the overall public health burden of the disease (5, 6). However, a lack of a proper vaccine or a sterilizing cure for the infection makes HIV one of the greatest public health threats of the 21st century.

Though the prognosis of HIV-infected people to AIDS has been largely reduced, the prevalence of other co-morbidities due to the virus has been steadily on the rise. Among them, HIV-associated neurocognitive disorders, or HAND accounts for nearly 50% of HIV-mediated complications. These are a subset of pathologies primarily associated with the central nervous system wherein affected individuals experience a gradual loss of neurological faculties which lead to motor problems, loss of sensory skills and memory, cognitive impairment etc. (7). Though severe forms of HAND have been mostly relegated to history due to antiretroviral therapy, milder

to moderate HAND continues to persist into the cART era (8). As a result, novel therapies aimed at preventing or treating these disorders of utmost importance from a perspective of public health.

2.0 HUMAN IMMUNODEFICIENCY VIRUS

2.1 HIV/AIDS Pandemic

Epidemiologically, the majority of the world's HIV-1 burden is borne by Sub-Saharan Africa (comprised of central, eastern, and southern Africa) accounting for 70% of all HIV-1 infections, globally (9, 10). The prevalence of AIDS-associated mortality has also been consistently high in Latin America, the Caribbean, and Central Asia. In addition, low- and middle-income countries account for more than 95% of new HIV infections (11). The demographic prevalence of HIV-1 infections in 2018 was roughly similar between men and women (~17.5 million as of 2018) (12). Besides, the incidence of HIV-1 is greater among African Americans than the Caucasian population (13).

HIV-1 is primarily a sexually transmitted virus that spreads through unprotected sexual intercourse. Due to the viremia that soon follows after the initial infection, exposure of broken skin or mucosal membranes to blood or blood products of an infected person can lead to potential transmission of the virus. Blood borne transmission is directly related to the viral copies in the patient's blood. A retrospective community-based Ugandan study found that the probability of transmission was directly correlated with blood viral index and transmission events were negligible in person with less than 1500 copies of HIV-1 RNA per ml of blood (14). Besides high loads of virus in blood plasma and CSF, it can also reach high titers in seminal and vaginal fluids 3-5 weeks post the initial onset of symptoms. Nonetheless, timely commencement of cART/HAART (combined antiretroviral therapy/highly active retroviral therapy) can greatly limit the shedding of viruses in blood plasma, cerebrospinal and reproductive fluids. A number of cohort

and ecologic studies have observed the suppression of viral shedding in bodily fluids, demonstrating the effectiveness of ART drugs. This reduction in viral load greatly depends on the choice of antiretroviral drug and its bioavailability in various anatomical sites, compliance to drug regime and extent of latent reservoir established by the virus (15, 16).

2.2 Virology of HIV

Human Immunodeficiency virus is an RNA virus belonging to the virus family *Retroviridae* and the known causative agent of Acquired Immunodeficiency Syndrome (AIDS) (17, 18). Historically, retroviruses have been grouped into three sub-families: *Oncornavirinae, Spumavirine*, and *Orthoretrovirinae*, of which HIV-1 is placed under the genera *Lentivirus* belonging to sub-family *Orthoretrovirinae* (19). Currently, HIV isolates are grouped into two distinct subtypes: HIV-1 and HIV-2. As discussed earlier, HIV-1 is the widespread and predominant cause of the ongoing epidemic. On the contrary, HIV-2 is restricted to certain parts of West Africa and certain isolates to other parts of the world including India and the United States. Besides their geographical disparities, people infected with HIV-1 tend to have robust and early progress to AIDS than their HIV-2 infected counterparts. Moreover, most HIV-2 infected people dichotomize into a category of 'long-term non-progressors or 'elite controllers, characterized by unusually high $CD4^+$-counts and negligible serum viral loads for several years (20-22). This makes HIV-1 more of a clinically relevant pathogen than HIV-2.

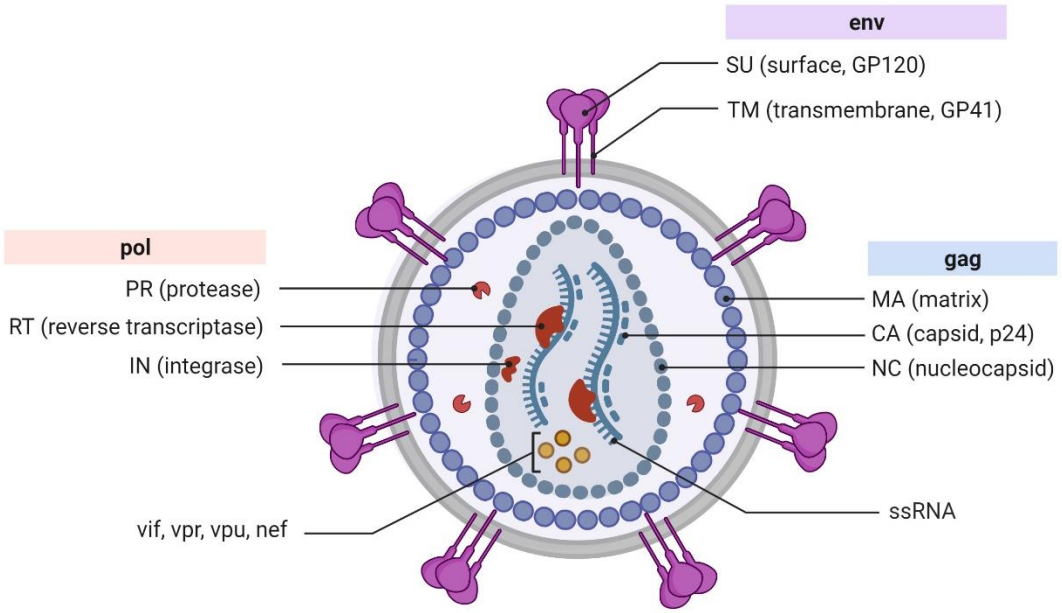

Figure 1: Structure of mature HIV virion

2.3 HIV-1 Genome

The genome of HIV-1 consists of two identical copies of single-stranded, positive-sense RNA of about 9.2 kb in length. The full-length genomic transcript of HIV-1 encodes three structural genes: *gag*, *pol*, *env* and other regulatory/accessory proteins as well. The *gag* encodes for four protein: p24 (capsid-CA), p7 (nucleocapsid-NC), p17 (matrix-MA) and p6, while *env* constitutes the glycoproteins of the viral envelope: gp120 (surface glycoprotein-SU) and gp41 (transmembrane glycoprotein-TM). While the *gag* proteins have a predominantly structural role, *env* proteins facilitate viral attachment and entry into the cell through cell surface receptor recognition. The three *pol* proteins, reverse transcriptase (RT), integrase (IN), and protease (PR), perform additional enzymatic functions responsible for viral replication, integration, and release respectively (23, 24).

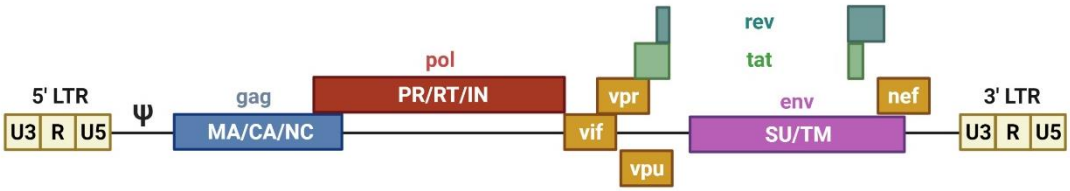

Figure 2: Schematic of the HIV-1 genome organization

2.3.1 Structural genes

Mature HIV-1 virions are enveloped retroviruses consisting of a conical capsid structure with an average diameter of ~145 nm. The capsid encapsulates two copies of a linear, single-stranded RNA and proteins required for infection, and subsequent integration (25). The fullerene-conical shaped structure of the capsid is attributed to the 1500 monomeric capsid (CA) proteins which are spatially arranged into hexamers and pentamers in a precise fashion giving the naked core its peculiar structure. The capsid, apart from its structural functions, also serves to protect the viral RNA from the host innate immune sensors and prevents its degradation. Additionally, it also plays a vital role in the transport and entry of the reverse-transcribed viral DNA into the host cell nucleus (26). The MA is a heavily myristoylated protein also encoded by the *gag* gene, found in close contact with the lipid envelope of the mature virion. It has been implicated in the targeted translocation of *gag* polyprotein to the cell membrane during budding and assimilation of *env* glycoproteins in nascent virus particles. *In vitro* studies have revealed that deletions and/or mutations to MA lead to misdirection of *gag* to intracellular compartments rather than the plasma membrane, further validating the role of MA in the HIV-1 life cycle (27, 28).

HIV-1 virions rely on their *env* proteins to succeed in infecting their target host cell. The envelope glycoproteins contribute to the narrow tropism of HIV-1 for T-cells, macrophages, and

dendritic cells. The lipoprotein envelope of HIV-1 consists primarily of glycoproteins gp120 and gp41 which span the entire membrane and also few additional host membrane proteins acquired during budding. Normally, gp120 recognizes CD4 expressed on circulating T lymphocytes and other cells like T-cell precursors, macrophages, DCs in the periphery. However, the virion also requires an additional chemokine receptor as a co-receptor for its unbridled entry into host $CD4^+$ cells (24). The chemokine receptors CCR5 and/or CXCR4, which are used by the virus to gain entry into target cells, also confer the cell tropism of HIV-1. Fundamentally, viruses that use the beta-chemokine receptor CCR5 are termed macrophage-tropic (or M-tropic/R5) viruses and have the ability to replicate in primary macrophages and T-cells. Conversely, viruses that prefer the alpha-chemokine receptor CXCR4 for entry are called T-lymphocyte-tropic (or T-tropic/X4) viruses and show a penchant for growth in primary $CD4^+$ T-cells but not macrophages (29). Both the R5 and X4 strains are not necessarily mutually exclusive and tend to co-exist during infection. Though R5 viruses prevail during the initial transmission and acute phase of infection, further change in tropism to an X4 variant often occurs. This change in co-receptor usage is often associated with a sharp decrease in $CD4^+$ T-cells and rapid progression to AIDS, lending credence to the fact that X4 viruses could be more virulent than their R5 counterparts (30). The two *env* proteins which are non-covalently linked, allow gp120 to solubilize in the plasma. This shedding of envelope glycoproteins during acute phase infection can thus serve as a diagnostic variable for detecting HIV-1 (31, 32).

2.3.2 Regulatory genes

As mentioned before, HIV-1 also encodes a complex collection of other supplementary proteins which are involved in a myriad of other functions required for viral infectivity and

survival. They are categorized as regulatory (*Tat* and *Rev)* and accessory genes (*Vpr, Vpu, Vif* and *Nef*) depending on their functions in the viral replicative cycle. *Tat* (also known as Trans activator of Transcription) is a trans-acting element that is thought to be essential for enhancing promoter activity and viral gene expression by over 1000-fold. HIV-1 proviral *Tat*-mutants demonstrate reduced levels of RNA and proteins *in vitro,* depicting the indispensable role of *Tat* in HIV-1 replication (33, 34). Similarly, *Rev* (also known as Regulator of expression of virion proteins) is a 20 kDa phosphoprotein expressed early on in the HIV-1 life cycle. Together with the *cis*-acting element termed as the *Rev*-responsive element (RRE), it functions to transport the unspliced viral mRNA to the cytosol through a special nuclear export machinery. RRE is a highly conserved, unique secondary structure located in the *Env* coding region of most known lentiviruses which binds to *Rev* and leads to the cytoplasmic accumulation of unspliced lentiviral transcripts which otherwise be targeted for splicing/degradation in the nucleus (35-37). Numerous *in vitro* mutagenesis and silencing studies have shown that mutations/deletions to *Rev* or RRE jeopardize viral protein synthesis and be detrimental to overall viral replication leading to the production of replication-incompetent viruses (38-42). Thus, these findings conclusively demonstrate the pivotal role of *Tat* and *Rev* in augmenting HIV-1 replication and infectivity.

2.3.3 Accessory genes

Apart from these regulatory genes, primate immunodeficiency viruses (HIV and SIV) also carry a unique array of accessory gene products necessary for creating a suitable host niche for efficient viral propagation and survival, in an otherwise hostile cellular environment (43). Under homeostatic conditions, viral entry and replication trigger a cascade of antiviral innate immune responses which targets specific mechanisms of the viral life cycle and prevents its completion.

These antiviral defenses include pattern recognition receptors (PRRs) like Toll-like receptors (TLRs), NOD-like receptors (NLRs), and components of the inflammasome (e.g., NLRP and ASC) etc. which upregulate interferon (IFN)/interferon-stimulated gene (44) expression and other classical NF-dB activated genes (e.g. IL-1β, TNF-α etc.). This drives both the infected and uninfected neighboring cells towards an 'antiviral state' and attracts immune cells to the site of infection leading to viral control and elimination (45). However, several viruses like IAV, EBOV, MABV, HTLV-1, etc. have evolved ways to evade and even exploit host innate defenses to ensure their persistence, dissemination, and effective transmission (46-48). Likewise, for this very reason, HIV-1 has also acquired accessory proteins to evade host immune responses and permit its unrestrained growth and spread inside the host (49). These proteins help downregulate host immunomodulatory molecules like MHC-I/II and CD4 (50), enhance the release of progeny virions through Tetherin antagonism (*Vpu),* induce G2-phase cell cycle arrest and modulate host cell oxidative metabolism favorably (*Vpr)* and inhibit cytosolic restriction/editing factors like APOBEC *(Vif)*, among other functions (43, 51-53). Altogether, these accessory proteins contribute to the improved pathogenesis of HIV-1 *in vivo.*

2.4 HIV-1 replicative cycle

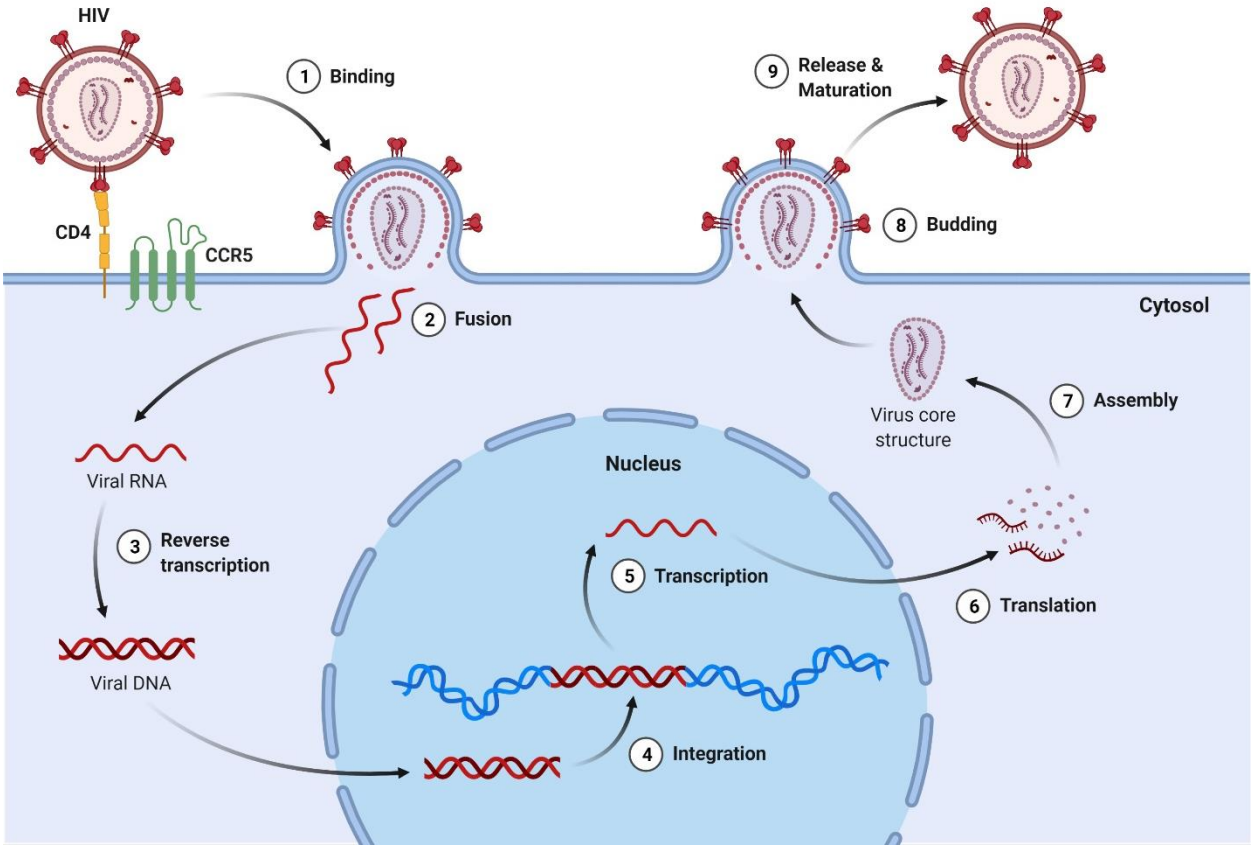

Figure 3: Overview of the HIV-1 replication cycle

2.4.1 Cell Entry

The first step towards any viral replication cycle is to gain access and entry into the host cell. In the case of HIV-1, it involves the binding of its surface gp120 to the CD4 receptor and a cognate co-receptor. The fusion of gp120 and CD4 results in a conformational change, exposing a conserved loop region that was previously buried inside. This allows for co-receptor binding and insertion of the gp41 transmembrane peptide into the host cell membrane. This results in membrane attachment/fusion and the delivery of viral contents into the cytosol (54). Once inside,

the uncoating of the capsid is initiated, which is thought to be a tightly regulated process and known to heavily influence the assembly of the reverse transcription complex (55) and other downstream processes. This stems from the observation that mutations in CA alter the processing of ssRNA to dsDNA and subsequent nuclear import, revealing a close relationship between HIV-1 uncoating and viral replication (56-58). Although the exact mechanism and spatiotemporal variables of capsid uncoating are ambiguous due to conflicting evidence (26), more recent studies suggest that capsid uncoating happens as a result of mechanical pressure due to the conversion of highly flexible ssRNA to a stable DNA duplex and occurs after the completion of first-strand transfer (50, 59).

2.4.2 Reverse Transcription

Reverse transcription and integration are defining characteristics of the members of the family *Retroviridae.* As uncoating proceeds, viral RNA is continually reverse transcribed to its dsDNA homolog by the RTC in the cytosol. Experimental proof by Drs. Baltimore and Temin about a viral enzyme that can convert RNA to DNA, supposedly violating the central dogma, were crucial in shedding light on the mechanism of HIV-1 replication and its persistence in infected hosts (60, 61). Reverse transcriptase is a 170 kDa heterodimeric RNA-dependent DNA polymerase (RdDP) enzyme containing two asymmetric subunits: p66 and p51. The p66 plays the enzymatic role and harbors the polymerase and the RNase H domains while the p51 takes on a more supportive structural role (62). After cellular entry, the reverse transcription is initiated by the binding of a lysyl-tRNA which primes the existing ssRNA strand, which is followed by minus-strand synthesis by the polymerase domain. Simultaneously, the RNase-H activity of RT degrades the corresponding RNA strand. The ends of the viral genomic RNA have direct repeat sequences

called R and this allows for the strand transfer of the negative-sense strand. As minus-strand synthesis and RNase H degradation proceed, a short sequence called the polypurine tract (PPT) resists cleavage and serves as the primer for the positive-sense strand synthesis. Following tRNA removal and another strand transfer reaction, the plus-strand synthesis occurs giving rise to double-stranded viral DNA ready for integration (63, 64). The completion of reverse transcription marks the formation of the pre-integration complex (PIC) required for inserting the viral DNA into the host genome as a provirus. As per conventional definition, the HIV-1 PIC is a molecular complex which no longer contains any traces of RNA and has integration-competent viral double-stranded DNA, which can efficiently merge into the host cell chromatin. The PIC, in addition, carries integrase and other host proteins in a highly compacted structure. This compaction is required for translocation into the nucleus through the small nuclear pore complex (65).

2.4.3 Integration

Once inside the nucleus, the viral integrase carries out perhaps one of the most critical steps in the entire replicative cycle. HIV-1 integration causes the perpetual transformation of the infected host cell and leads to the establishment of a proviral reservoir. The resulting persistence of the integrated viral reservoir in the cell makes any chances at a sterilizing cure for HIV-1 infection implausible (66). HIV-1 integrase is a multidomain enzyme encoded by the *pol* portion of the genome. Expression of *pol* occurs as a *gag-pol* polyprotein through a programmed ribosomal frameshift; this is required since *pol* is in a different ORF than *gag* and cannot be translated without this frameshift (67). The integrase has three heterogenous domains, the amino-terminal domain (NTD), catalytic core domain (CCD) and the carboxy-terminal domain (CTD). While the NTD and CCD play a DNA binding role, the CCD holds the catalytic triad motif with the

polynucleotidyl transferase activity required for strand transfer (68). After nuclear entry, the 3' ends of the viral DNA are processed to remove two nucleotides by the PIC. Following 3' end processing, strand transfer ensues which joins the 5' ends of the viral DNA to the host target DNA. The single-stranded nicks are sealed by the cellular DNA repair machinery which completes the DNA recombination process (69). Though HIV-1 integration might seem very stochastic, in actuality, it is a highly specific and regulated process. Studies have observed that HIV-1 prefers to integrate into transcriptionally active sites and dense, gene-rich loci. Also, HIV-1 seems to target the regions of euchromatin in the nuclear periphery rather than chromatin found deep inside (70-73). As a result, successful integration of the viral genome ensures sustained viral gene expression and high levels of viremia in the patient's plasma unless intervened by ART.

2.4.4 Virion egress

The final step towards producing a functional, mature virion is viral egress from the infected host cell. HIV-1 exits the cell as immature virus-like particles (VLPs) by budding through the cell membrane. Much of the viral budding process is coordinated by the *gag* protein which orchestrates the trafficking of the required viral and host factors towards the plasma membrane and their assembly into immature virions. This also includes directing the *env* proteins towards the cell membrane and packaging the two RNA strands (74). The *gag* protein also holds docking domains for the ESCRT (Endosomal sorting complex required for transport) complex which facilitates the nicking of the fully budded viral envelope. Specifically, HIV-1 triggers the activity of the ESCRT-III complex and also requires only a subset of these host factors to complete its morphogenesis. (75, 76). Following the release of the immature VLPs, the viral proteins need to be processed to complete the maturation process to generate infectious viruses. HIV-1 protease is

a homodimer aspartyl protease that cleaves *gag* and *gag-pol* polyproteins to generate mature structural proteins. (77, 78). The proteolytic processing redefines the structural morphology of the capsid. Immature *gag* molecules are arranged radially and in close association with the envelope but reassemble into the distinct conical capsid structure as a result of the protease action (79). This mature HIV-1 virion can now go on to infect bystander cells and progress the infection. Considering its paramount importance concerning the viral life cycle, HIV-1 proteases have thus emerged as lucrative targets for chemotherapy.

3.0 HIV-ASSOCIATED NEUROCOGNITIVE DISORDERS

3.1 HIV-1 replication and persistence in CNS

The central nervous system is a unique anatomical structure that is sequestered from the rest of the peripheral vasculature by the blood-brain barrier (BBB). This highly vascular, semi-permeable structure tightly governs the movement of ions, molecules, etc. between the blood and CNS. This helps regulate CNS homeostasis and prevent its exposure to microbes, toxins etc. (80). Though the BBB is impregnable to toxins and most drugs, viruses like HIV-1 have evolved varied modes of entry into the CNS. Accumulating evidence suggests that HIV-1 enters the CNS as a stowaway via an infected monocyte or as cell-free virions through endothelial transmigration (81, 82). Regardless of the route of entry, the viral particles go on to productively infect the perivascular macrophages lining the BBB which ultimately result in the infection of microglia. The diminished bioavailability of cART drugs in the central nervous system due to ineffective BBB penetration encourages the establishment of persistent infection through long-term viral reservoirs (83). This theory is corroborated by studies that show the presence of HIV-1 RNA in CSF of HIV-1 positive patients receiving cART who are otherwise plasma negative, indicating the low-level of virus replication in the brain despite antiretroviral therapy (84-86). Besides, the immune privilege and longevity of glial cells in the CNS microenvironment are also considered to be possible explanations for HIV-1 latency in the brain. Human brain microglia have a long-life span with low turnover rates than other immune cells in the periphery (monocytes, macrophages, dendritic cells etc.) (87). Shielded from the immune system due to the surrounding blood-brain barrier, these long-lived microglia and surround glial tissue are conducive for infection and establishment of a

stable cellular reservoir in a rapid manner in the initial phases of the infection (87). Furthermore, these reservoirs become the focal points of CNS HIV-1 infection and help reseed peripheral viral titers.

3.2 HIV and neurodegeneration

While HIV-1 is commonly associated with T-cell lymphopenia and immunosuppression, it is important to acknowledge the involvement of the central nervous system, especially the brain. This impact on the CNS and its affiliated faculties is collectively called the HIV-associated neurocognitive disorders or briefly as HAND. Clinically, HAND is classified into three categories depending on the extent of neurological involvement: asymptomatic neurocognitive impairment (ANI), mild/moderate neurocognitive disorder (MND) and HIV-associated dementia (HAD) (88). HAND is a progressively debilitating disorder that involves a constellation of symptoms ranging from deterioration of motor skills, impairment of cognition and verbal fluency, behavioral changes, dementia and even death (89). In the pre-cART era, the extent of neurodegeneration was very explicit with the rapid progression of HAND into HAD. However, the advent of mono-therapeutic and subsequent combination ART successfully halted the prognosis of HIV-neuropathy to severe dementia (8), besides the reduction of overall HAND incidence (by up to 75%) as well. (90). While significant inroads have been made regarding HAND pathogenesis in the CNS, the development and approval of effective chemotherapeutics to treat this condition remain at large.

3.3 Factors in HAND progression

Our current understanding of HAND pathogenesis outlines a shared combination of both viral and cellular factors and their culpability in facilitating HIV-1 neuropathogenesis, as outlined in Figure 4. While neurons are not permissive for HIV-1 entry and replication, they are susceptible to the neurotoxic effects of several virally encoded proteins. For instance, gp120 has been investigated and documented for its notorious neurotoxic capacity (91). Specifically, transgenic mice expressing gp120 display neuronal and glial aberrations similar to those observed in the CNS of HIV+ patients (88).

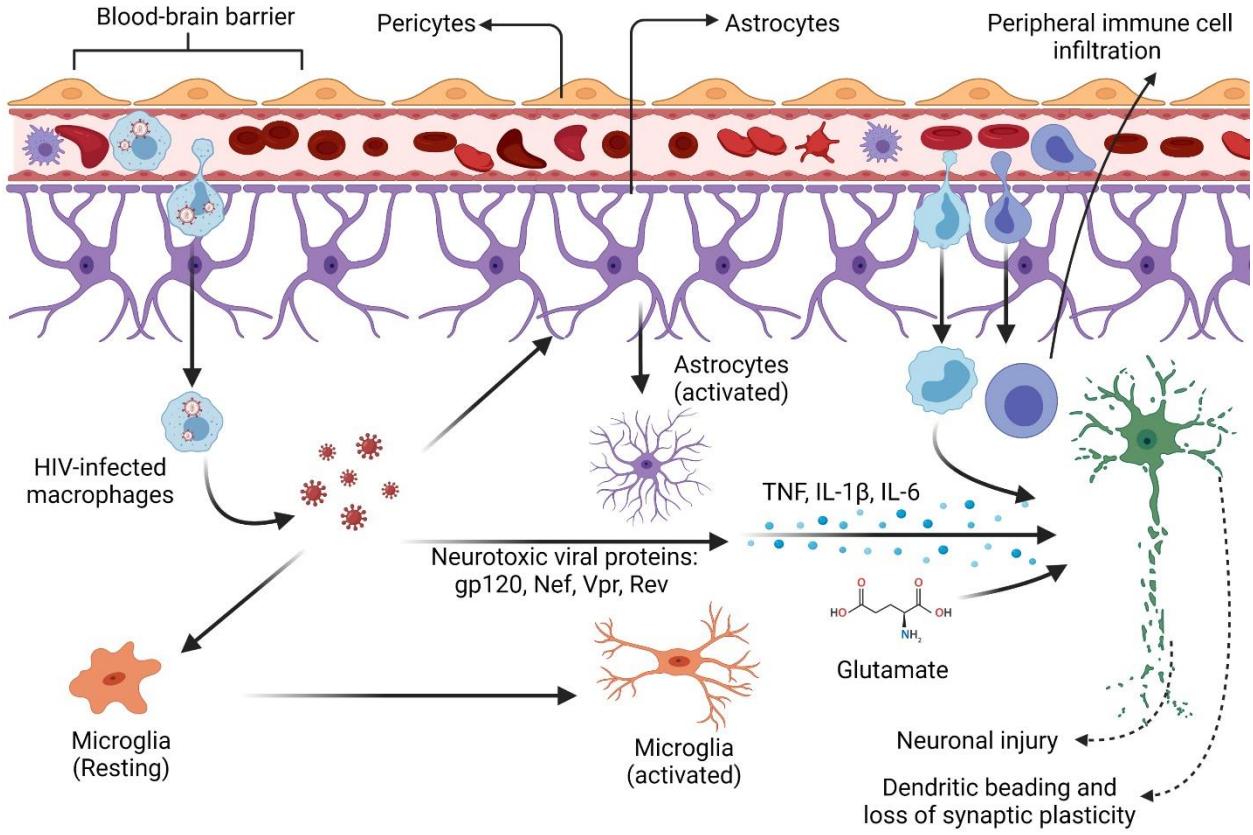

Figure 4: Factors contributing to the neuropathogenesis of HAND

Also, gp120 leads to neuronal cell death through excessive $Ca2^{+}$ influx via cell permeabilization and CCR5/CCX4 mediated apoptosis (92-94). Similarly, instances of Tat (a regulatory protein) mediated neurotoxicity have also been reported through calcium-induced neurotoxicity, similar to that of gp120 (95, 96). Other evidence also indicates that Tat leads to neuronal dysfunction by interfering with dopamine reuptake and signal transduction (97). Besides the viral factors, other host-related factors have also been implicated in HIV-1 neuropathogenesis. The host response to HIV-1 in the CNS is comprised of the release of pro-inflammatory cytokines and chemokines such as TNF-α, IL-1β, IL-6, CCL2, CXCL12 and release of other neurotoxic chemicals like glutamic acid, Nitric Oxide, Quinolinic acid etc. (98). This inflammatory milieu serves to further activate the immune cells in the brain while also recruiting additional naïve macrophages from peripheral sites. This burgeoning positive feedback loop results in a state of abnormal, hyperimmune activation which damages neurons and the surrounding glial cells causing gradual neurodegeneration and its associated pathologies seen in HAND.

3.3.1 Role of microglia in HAND development

Microglia are resident phagocytes of the human central nervous system, accounting for nearly 15% of the total cell population in the human brain (99). While the functional neuronal cells are derived from the neuroepithelium, microglia, on the contrary, are derived of mesodermal origin. These cells originate from the embryonic yolk sac which then leaves and populates the fetal CNS during embryonic development (100). These sentient cells constantly scan the brain parenchyma for antigenic stimuli and once activated, become the focal points of the host immune response in the CNS. Genetically, microglia are a class of macrophages and are, therefore, naturally conducive for HIV-1 infection (101). Innate immune cells such as microglia and

macrophages employ a range of pattern recognition receptors (PRRs) to detect the presence of antigenic and potentially infectious stimuli called pathogen/damage-associated molecular patterns (PAMP/DAMP). These PRRs which include Toll-like receptors (TLR), NOD-like receptors (NLR) etc. are activated upon contact with their cognate antigenic ligands and induce the expression of key genes required for host innate immune response (102). The classical model of microglial activation involves a resting (M0) state and two polarizing activation states with distinct functions: pro-inflammatory (M1) and anti-inflammatory (M2) states. While the latter is involved in immunoregulatory and neuroprotective functions, the former is generally considered to have a neurotoxic function due to its role in promoting inflammation (103). Upon HIV-1 infection, resting microglia are activated by exposure to viral PAMPS like cytosolic/uncapped RNA, HIV-1 proteins like gp120, Tat etc. This activation results in a large-scale secretion of pro-inflammatory cytokines (TNF-α, IFN-α, IL-6, IL-8, IL-1β etc.) and chemokines (CCL2, CCL5, Fractalkine etc.) which drive the immune response to the virus in CNS (104-106). This immune locus also attracts other immune cells from distant sites of the body which cross the BBB and promote further inflammation. Inadvertently, however, the neurons and surrounding glial tissue suffer collateral damage from this exacerbated response. Consequently, this leads to synaptic pruning, dendritic beading etc., which are considered to be telltale signs of neurodegeneration and HAND.

3.3.2 Role of microglia-derived cytokines/chemokines in HAND development

While the microglia are important in driving HAND; at the molecular level, however, it is carried out by the inflammatory molecules which they secrete into the extracellular space. Cytokines are small peptide molecules of approximately 5-20 kDa, involved in an array of cell signaling and transduction processes (102). Among their many functions, they are primarily

immunomodulatory agents involved in the induction and further sequelae of host immune response (107). Normally, these cytokines and chemokines are favorable for host homeostasis. However, during HIV-1 infection, these chemicals are implicated in the pathogenesis of the virus. This becomes particularly important when there is neurological involvement during the course of the infection. Prior studies have revealed that the CNS microenvironment during HIV-1 infection is predominated by several inflammatory molecules as a direct consequence of the virus or its gene products. For example, TNF-α production is induced in response to the presence of virus proteins, gp120 and Tat (108). The latter has also been known to influence the secretion of IL-6 and Il-8 in astrocytes (109). TNF-α is known to promote BBB permeability by upregulation of key cell adhesion and chemoattractant molecules like intercellular cell adhesion molecule-1 (ICAM-1), Fractalkine ligand (CX3CL1), MCP-1 among others leading to increased influx of peripheral monocytes and macrophages (110-112). Besides, TNF-α can also act directly as a neurotoxic stimulus; it has been known to overstimulate NMDA receptors of neurons and causing increased secretion of glutamate (an amino acid) from neurons and astrocytes, leading to excitotoxicity (113, 114). This is evidenced by elevated CSF levels of this amino acid in HIV+ patients with neurological symptoms (115-117). Similarly, IL-6 and IL-8 have also been suggested to directly aid in virus replication (118-121). On the whole, this suggests the importance of these microglial derived cytokines and chemokines in abetting HAND development in HIV positive patients.

4.0 MICRO RNAs

4.1 Non-coding RNAs

Since the discovery of small non-coding RNAs in the early 1990s, the field of microRNA biology has exploded tremendously, with new insights into the role of these non-coding RNAs in the function and development of biological systems being gained every day. Consequently, research into the possible dual functions of these small RNAs in aiding both prognosis and amelioration of systemic diseases has gained momentum. Additionally, the successful completion of the human genome project (122, 123) has supplied new knowledge into the previously enigmatic role of the non-coding regions of the human DNA. This has shifted the conventional perspective of biomedical scientists from overlooking these 'junk DNA' and considering a much deeper purpose in the normal functioning of organisms. Current estimates suggest that the majority of the cellular DNA and RNA pool (up to 97-99%) is made up of non-coding nucleic acids, whose nonfunction can lead to a variety of pathological states in the host organism (124).

At any given time, a eukaryotic cell expresses several different kinds of RNA, each with its specific functions. A class of RNAs called non-coding RNAs (ncRNA) comprise the bulk of the total cellular RNA, with the exclusion of messenger RNA (mRNA), which directly encode for host proteins. These ncRNAs are conventionally categorized based on their size or functionality; they can be either small (18-200 nucleotides) or large (>200 nucleotides) and can serve both housekeeping and regulatory roles. The housekeeping ncRNAs, although they don't code for any proteins, aid peptide biosynthesis indirectly in the form of ribosomal RNA (rRNA) and transfer

RNA (tRNA) (125). On the contrary, the regulatory ncRNA include the micro RNAs (miRNA), small interfering RNAs (siRNA), small nuclear RNA (snRNA) small nucleolar RNA (snoRNA), piwi-interacting RNAs (piRNA), and long non-coding RNA (lncRNA). However, these distinctions become blurred due to the 'moonlighting' function of most of these RNAs. Nonetheless, these RNAs have clearly defined roles in modulating cellular protein expression, metabolism etc. whose failure results in disease progression (126). Their proven roles behind several disorders make them lucrative candidates as biomarkers, therapeutics etc.

4.2 MicroRNAs and RNA interference

Maintenance of cellular homeostasis is cardinal to the normal growth and development of any living organism. A fine balance between anabolic and catabolic processes exists, as a result of several host factors and any change can prove to be detrimental. Multiple regulatory factors exist in eukaryotic organisms to regulate the levels of gene expression. These constitute regulatory pathways that occur either epigenetically, co-transcriptionally or post-transcriptionally. Epigenetic or co-transcriptional pathways alter the stoichiometry (i.e., total number) of RNA transcripts thereby altering the expression of its associated gene products. The modalities associated with them is beyond the scope of this review; however, some excellent journal articles highlighting these can be found here (127-129).

At any given time, a typical mammalian cell has upwards of 100,000 mRNA transcripts encoding a myriad number of proteins. Due to the vast quantity of RNA information, post-transcriptional regulation is not merely a stochastic process, but rather a strictly maintained one

with elaborate mechanisms involved. Non-coding regulatory RNAs such as miRNAs, siRNAs are one such highly studied host-regulatory factors and form a unique branch of RNA biology. These short RNAs employ sequence-based recognition to identify and target host messenger RNA and modulate gene expression, both positively and negatively, in a process collectively known as RNA-mediated interference (RNAi).

RNAi, also known as post-transcriptional gene silencing (PTGS) is a complex, biological phenomenon wherein small non-coding RNA (sncRNA) sequences bind to host mRNA, resulting in transcript degradation and subsequent downstream translational repression. These sncRNAs may either be of exogenous and endogenous origin which give rise to siRNA and miRNA, respectively. Though the primary function of both these RNAs is to modulate host gene expression, they have distinct origins and purpose. Small interfering RNA (also known as siRNAs) are 20-23bp long, RNA duplexes exhibiting perfect complementarity to the targeted gene transcript of interest. These RNAs are mostly derived exogenously, i.e. from the extracellular environment such as viral RNA, transposons, transgenes etc. and serve to protect the integrity of the host cell by repressing the expression of foreign/invasive nucleic acids (130). Contrarily, microRNA are endogenously derived nucleic acids which have multiple translational targets owing to their partial sequence complementarity. As a result, a single microRNA can abbreviate the effects of multiple genes making them lucrative targets in scientific research.

4.3 miRNA biogenesis

Synthesis of miRNA begins with the transcription of primary precursor miRNA (pri-miRNA) by host RNA polymerase II. This pri-miRNA is either co-transcriptionally or post-transcriptionally processed by enzymes DGCR8 and Drosha into 700-100 bp precursor miRNA (pre-miRNA) (131). These hairpin structures are exported into the cytosol by Exportin-5/Ran-GTPase complex (132), where further processing into mature ds-miRNA is done by the ribonuclease Dicer (133). This mature miRNA duplex is then actively loaded on to the miRNA-induced Silencing Complex (RISC), which is composed of the Argonaute (AGO) family of proteins (134). The thermodynamically stable guide strand is selected which is then unwound from the passenger strand, with the latter being degraded (135). This partial-complementary miRNA sequence is then involved in the translational repression of multiple mRNAs and their corresponding genes. The overall schematic of miRNA biogenesis is depicted in the figure below.

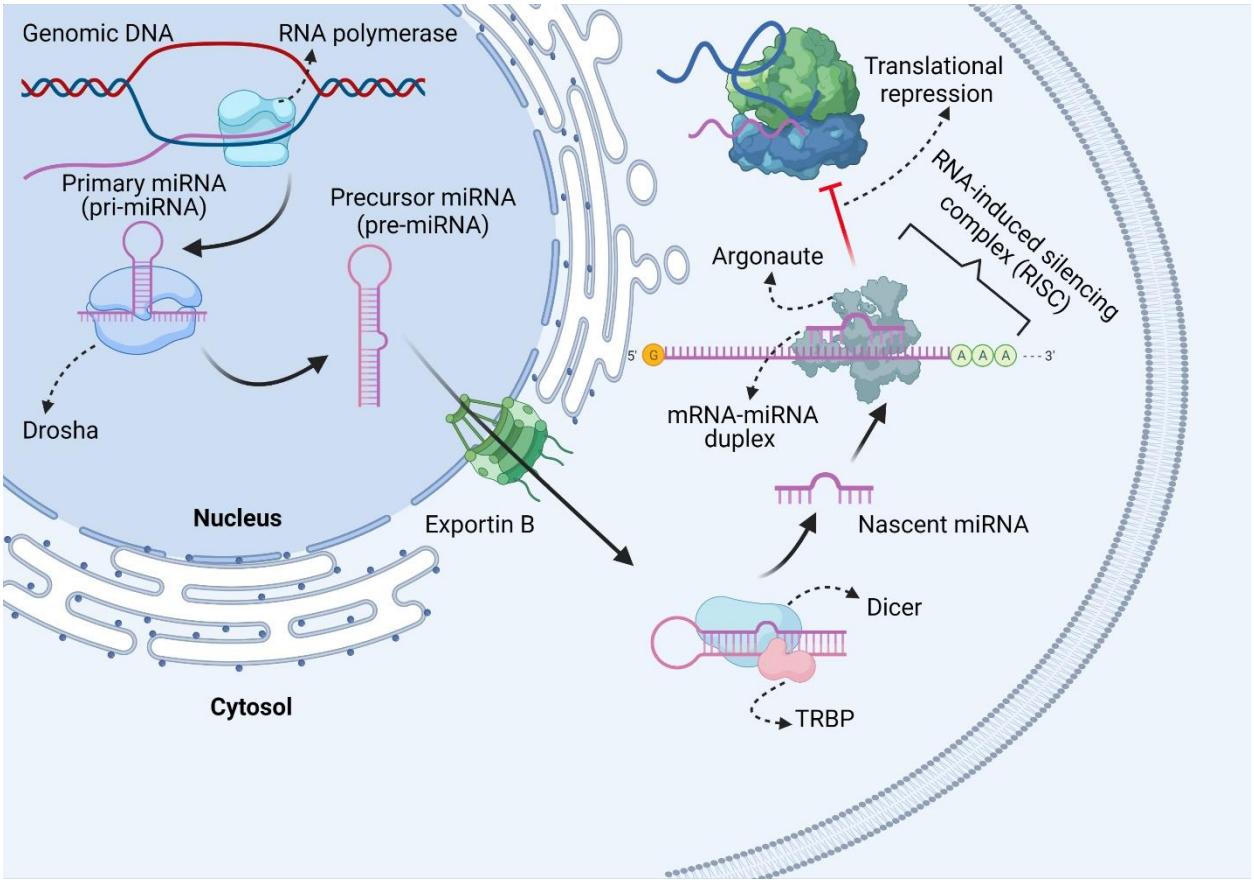

Figure 5: Schematic of miRNA biogenesis and RNA interference

4.4 Therapeutic potential of miRNAs

As summarized in the table below, the dysregulation of key miRNA genes is involved in the etymology of various diseases. Therefore, it is only logical to hypothesize the potential therapeutic usage of these miRNAs through evidence-based manipulation in biological systems. However, the trajectory of miRNA-based therapeutics in successful clinical use has been marred with difficulties, partly owing to the lack of proper research into their functionalities and biological

effects. Several studies have pointed out the differential expression of these miRNAs in a plethora of maladies, as summarized in the following table.

Table 1: Differential expression of miRNAs and their associated diseases

Signature miRNA	*Disease*	*Reference(s)*
miR-10b, miR-34a, miR-124, miR-181 etc.	Glioblastoma multiforme	(136-138)
miR-155-5p, miR-130b	Kidney Stones	(139, 140)
miR-122	Hepatitis C	(141, 142)
miR-375, miR-200c	Gastric Cancer	(143, 144)
miR-34a	Diabetes	(145)
miR-96, miR-211 etc.	Retinopathy	(146, 147)
miR-145, miR-33	Atherosclerosis	(148, 149)
miR-433	Myeloproliferative Disorder	(150, 151)
miR-122, miR-21, miR-223	Hepatocellular carcinoma	(152, 153)

Altogether, these present pressing evidence for the research and development of miRNA-based therapeutics. Broadly speaking, these therapeutics are divided into two categories: miRNA mimics and miRNA antagonists. miRNA mimics, as the name suggests, mimic the function of endogenous miRNAs. These mimics are synthetic oligonucleotides resembling the host miRNA of interest and are used to substitute the diminished function of target miRNAs, in the event of a disease or injury. miRNA antagonists, also known as antagomirs/antimirs are antisense oligonucleotides that exhibit complementarity to target miRNAs and degrade them (154). Naked RNA is degraded in biological fluids rapidly due to the ubiquitous presence of ribonucleases. As

a result, successful application and delivery of these systems require the use of chemical modifications to these oligoRNAs to extend their half-life and bioavailability. Several modifications such as the addition of an O-methyl, 2-methoxyethyl, phosphorothioate functional groups have been proposed with some success (155, 156). However, these modifications are tolerated till a threshold before the loss of *in vivo* activity is observed (156).

Another constraint towards the successful development of miRNA therapeutics is the efficient and targeted delivery of these oligoRNAs to the organ of interest with minimal side effects. Multiple modes of delivery have been proposed which included either viral or non-viral modes of delivery. While viral vectors employ adenoviral/lentiviral vectors to introduce these exogenous oligonucleotides, non-viral techniques employ chemical vehicles to deliver our gene of interest. Usage of viral vectors remains controversial due to the ever-present safety issues associated with them. Non-viral delivery systems typically use lipid excipients which have a natural tendency to interact with the hydrophobic cell membrane of animal cells. These include the use of poly (lactide-co-glycolide) (PLGA), synthetic polyethyleneimine (PEI), cyclodextrin, Polyethylene glycol (PEG) among others. Though toxicity, non-specific cellular uptake, and anaphylaxis are major obstacles to be considered, multiple studies have indeed reported significant inroads regarding miRNA delivery systems (157).

The majority of present knowledge regarding these delivery systems was obtained as a result of research in siRNA therapeutics, with the first siRNA-based drug Patisiran gaining FDA approval in 2018, for the treatment of hereditary transthyretin-mediated amyloidosis. (158). One of the preliminary miRNA-based therapy candidates to enter the drug development pipeline was Miravirsen/SPC3649 developed by Santaris Pharma. This phase-II clinical trial candidate utilizes an LNA-antisense approach and targets the 5’-end of miR-122. This miRNA, which is highly

expressed in the liver, was found to be indispensable for HCV replication through interaction with the 5' end of the viral genome (142). Initial phase-IIa trials using Miravirsen reveal a dose-dependent reduction of viral replication, with minimal adverse effects (159). Miravirsen is one of the many potential miRNA-based therapeutic candidates currently under clinical development. This shows promise of the still untapped potential of miRNA-based therapies in treating infectious and chronic conditions.

4.5 Selection of candidate miRNAs and significance in HAND

The candidate miRNAs, miR-20a and miR-106b among others, were identified through a global transcriptome analysis in a previously published study from our group (160). Briefly, mRNA and miRNA profiles from PBMCs of HIV-1 seropositive individuals with varying degrees of neurocognitive impairments (MND and HAD) were compared with HIV-1 negative individuals belonging to the Multicenter AIDS Cohort Study (MACS). By employing a unique systems biology approach, differential expression of multiple miRNA targets was revealed. In particular, miR-20a and miR-106b were found to be upregulated in HIV+ neuroimpaired patients. These miRNAs are thought to affect TNF-α, IL-1β, IL-6 among other cytokines by targeting FOXO1, NOTCH signaling pathways. As a result, these miRNAs could serve as lucrative targets for research into their role and therapeutic usage in ameliorating HAND.

5.0 3D BRAIN ORGANOIDS

5.1 Human Brain

The brain is arguably one of the most complex structures in the animal kingdom which has piqued the scientific curiosity of philosophers and scientists for several centuries. With its 100 billion neurons and trillions of synapses, it is the source of all cognition and intelligence. Of the animal species, particularly hominids, humans enjoy an elevated sense of intellectuality and perception. Thanks to millions of years of evolution, this has granted humans the highest encephalization quotient (EQ), more than any other animal on the planet (161). While our current knowledge of CNS mostly relies on cadaver tissue explants, animal models, neuroimaging etc., highs cost and low feasibility associated with them hinder scientific progress. As a result, novel *in vitro* models which have a high degree of physiological relevance is exigent, thus making research into 3D organoids an exciting research avenue.

5.1.1 Evolution of cell culture and organoids

Much of our present knowledge about the field of neurobiology is through research from post-mortem examinations of humans and experimental studies on mice and other non-human primates. However, constraints and ethical issues associated with these methods prompt us to find novel models to investigate neurobiological phenomena. This combined with the modern breakthroughs in stem cell technology and bioengineering has enabled the generation of three-dimensional (3D) organoids of the brain which show great promise in accentuating our

understanding of the human nervous system and serve as a benchmark tool to study neuropathological and psychiatric morbidities. The seminal work of Dr. Harrison on the growth of neurons from frog embryo grafts marked the advent of animal tissue culture (162). However, difficulty in handling primary tissue cultures and the constant need for fresh tissue was superseded by the introduction of immortalized cell lines. This polished the *in vitro* culture of mammalian cells and have conferred consistency and reproducibility to biological studies. Furthermore, their self-renewal potency, ease of manipulation and usage have led to fundamental breakthroughs in the fields of cancer biology, developmental biology etc. With regards to neuroscience, multiple culture techniques of neurons from different animal and insect species have been developed over the years, which have lent insights into basic biochemical and life-sustaining processes of the central nervous system (163-168). However, primary neuronal cultures still suffered the shortcomings as other forms of primary culture like reduced feasibility of maintenance and repeated need for tissue explants. Also, the homogeneity of the cultures meant that *in vivo* cellular cross-talk and interaction between different cell types in the CNS niche could not be reproduced and examined. Subsequently, the emergence of human embryonic stem cells (ESC) (169) and induced pluripotent stem cells (iPSC) (170, 171), together called the human pluripotent stem cells (HPSC) was viewed as a great leap forward in biomedical science. Their pluripotency permits them to be directed towards any germ layer and cell fate which allowed for greater physiological relevance of future studies as tissue-specific cellular architecture could be replicated *in vitro* (172). These HPSCs modelled diverse and unrelated cell types like cardiomyocytes, neurons, pancreatic islets etc. and show appropriate functional utility. For instance, knowledge of embryonic neural development has allowed for effective iPSC mediated neocorticogenesis through directed external cues (173, 174). Besides, patient-derived IPSCs for several hereditary diseases like Parkinson's

disease, β-Thalassemia, Gaucher's disease, Down's syndrome etc. have been developed which aid in the better appreciation of genetic and epigenetic mechanisms underpinning these disorders (175, 176).

Despite their obvious advantages like scalability and optimized differentiation methods, two-dimensional cultures of pluripotent stem cells fail to recapitulate the anatomical intricacies and the functional complexity of the central nervous system (177). Additionally, the fetal origin of ESCs shrouds its usage in ethical controversies (178). This warranted the development of a model which captured the three-dimensional cytoarchitecture of organs while maintaining its relevance to human physiology, albeit on a microscopic scale. Thus, with existing iPSC lines and novel differentiation protocols, three-dimensional cultures resembling organs, popularly called 'organoids' were developed.

5.2 Neural Organoids

The field of organoid biology, especially brain organoids is fairly new, with the first 3D cerebral organoids being developed just a few years ago (179). Since then, multiple organoid protocols with diverse cell compositions have been published. Initial efforts involved self-organizing neural tube-like structures under serum-free conditions, which allowed for neural, astroglial and oligodendroglial differentiation (173). Eventually, multiple studies involving neural rosettes were published, whose cellular organization is reminiscent of early neurogenesis i.e. NEC and radial glial cells displaying apical polarity enveloping a fluid-filled ventricle (180-182). This speaks to the inherent self-organizing tendency of iPSC-derived neuroprogenitor cells which were

able to resemble both the spatial arrangement and temporal differentiation patterns of the developing neocortex as evidenced by their molecular markers. Later, altered media components and directed extrinsic cues were used to develop a 'serum-free culture of embryoid body-like aggregates with quick aggregation' (SFEBq) (183-186), as a variant to conventional embryoid cultures (187). These modified embryoid cultures were seen as a considerable improvement to their 2D equivalents as they translated the spatiotemporal aspects (e.g., progenitor population, the sequential genesis of neurons etc.) of the two-dimensional cultures in 3D. Some of these SFEBq cultures also mirror multiple aspects of *in vivo* neurogenesis such as zonal partition (VZ, SVZ, IZ), apical-basal polarity, rostral-caudal patterning etc. (183, 184). Successive alterations to SFEBq cultures led to the development of the first cerebral or 'whole-brain' organoids (179). These organoids displayed a variety of discrete brain region identities (forebrain, hindbrain, hippocampus, choroid plexus, retinal cup etc.) and also exhibited cortical organization similar to the developing neocortex. These organoids were cultured by immersion in Matrigel which provided an extracellular scaffold for robust tissue growth. Similar contemporary studies demonstrated the significance of an extracellular matrix (ECM) for proper tissue development and neuroepithelial polarization (183, 188, 189).

Subsequent protocols aimed at amending the fidelity of cortical organoids as one major constraint towards optimized organoid production are the rampant issues concerning its variability and irreproducibility. However, recent studies have begun to overcome these challenges in refining the consistency of organoid cultures. Notably, a small-scale spinning bioreactor was used to generate reproducible fore-brain organoids displaying all six cortical layers with a distinct outer radial glial cell layer (190), which is a distinct feature of the developing human cortex (191). Similarly, other organoid techniques have managed to achieve moderate to high reproducibility

and reduce variability between batches (192-194). While the prior approaches relied solely on the intrinsic self-assembling ability of HPSCs, lately the focus of organoid farming has also shifted towards establishing region-specific identities. These guided methodologies use patterned external cues to drive differentiation towards desired lineages (195). A plethora of protocols have thus far been published on spawning organoids that resemble different regions of the brain such as the midbrain (190, 196-198), hypothalamus (190, 199), cerebellum (200, 201), pituitary (202-204), hypothalamus (190, 202) and retina (185, 205, 206).

5.3 Organoids and neurodegenerative disorders

Organoids have emerged as an extremely valuable tool to model neurodevelopmental and degenerative disorders due to their ability to faithfully recapture important aspects of the human brain and CNS development. The lack of a 3D microenvironment of planar cultures and the tenuous physiological relevance of animal models have made brain organoids alternative candidates in neurobiological and cancer research. Preliminary efforts to model neurological abnormalities involved the serum-free culture of whole-brain organoids to study microcephaly (179). Subsequently, the use of brain organoids has gathered momentum with various neurodevelopmental and psychiatric disorders being modelled.

5.3.1 Limitations and future of brain organoid technology

Like any other experimental model, organoids too suffer some drawbacks in their ability to capture the physicochemical environment of the brain and have major feasibility issues while

doing so. While the field of organoid technology is relatively new, consistent research has resulted in an expanse of knowledge throughout the past few years. However, further improvements are needed to address the inherent issues carried by these organoids to effectively mimic mammalian neurogenesis and establish 3D cultures as forerunners in modelling neurological disorders. Heterogeneity between batches poses a major constraint in multiplexing organoid cultures. Sequencing analyses have revealed batch-to-batch variabilities that plague organoid cultures, in part due to differences in the bio-reactor conditions and cell composition between batches (192). Also, the lack of proper patterning cues in most early organoid protocols and reliance on self-organization contributed to the reproducibility issues of three-dimensional cultures. As a result, there was a desperate need for protocols that utilize controlled differentiation and bioreactor conditions to reduce variability and impart homogeneity to brain organoids (207). A novel, miniaturized, spinning bioreactor unit called the SpinΩ was used to generate fore-brain organoids which ameliorated the batch disparity issues providing the future opportunity for scalable and economical 3D tissue cultures. (190). Further refinement of existing techniques and quality control practices would substantially increase the fidelity of organoids and their disease models.

6.0 HYPOTHESIS AND AIMS

As mentioned earlier, prior findings from our laboratory have indicated the presence of differentially regulated miRNAs in HIV+ HAND+ compared to HIV+ HAND- patients. Furthermore, downstream analysis revealed their possible role in influencing cytokine secretion and other inflammatory pathways. This combined with the fact that microglia are focal immune responders to HIV-1 in the CNS environment led us to our hypothesis: human microglia primed to overexpress these candidate miRNAs of interest could protect against HIV-1 infection and HIV-mediated neuroinflammation. To do so, we generated microglia overexpressing selected candidate miRNAs of interest through lentivirus transduction. Using these stable microglial cell line(s), we eventually planned to examine their response to sterile and infectious inflammation through the following specific aims:

Aim 1: Generation of stably transduced microglia expressing candidate miRNAs of interest and 3D organoids using human neuroprogenitor cells.

- Generate lentiviruses encoding candidate miRNAs through transfection of 293T cells.
- Generate stably transduced microglia expressing candidate miRNAs and perform puromycin selection.
- Confirm successful lentiviral transduction and insertion through genomic PCR and validate newly established stable cell line through flow cytometry and fluorescence microscopy.
- Evaluate the effect of multiple stimuli in driving astrocyte differentiation in immortalized human neuroprogenitor cells and 3D brain organoids.

Aim 2: Investigate the anti-inflammatory effects of candidate miRNAs and their subsequent role in preventing HIV-1 replication and HIV-mediated inflammation in stably transduced microglia.

- Evaluate the effect of miRNA expressing microglia in reducing immune activation in the presence of common TLR stimuli like LPS.
- Evaluate the effect of miRNA expressing microglia in reducing HIV-mediated inflammation.
- Evaluate the effect of miRNA expressing microglia in modulating HIV-1 replication through flow cytometry, fluorescence microscopy and virus titer assays.

7.0 MATERIALS AND METHODS

7.1 Cell Culture

Human Embryonic Kidney (HEK) 293T, U87MG $CD4^+$ $CCR5^+$ and immortalized HMC3 microglial cells (ATCC® CRL-3304) were cultured in 37 ^oC and 5% CO_2 in Dulbecco's Modified Eagle Medium (DMEM) (Lonza Biosciences) supplemented with 10% Fetal Bovine Serum (HyClone^{TM}), 1% L-glutamine (Gibco^{TM}) and 1% Penicillin/Streptomycin (Gibco^{TM}). Human immortalized neuroprogenitor (ReN) cells were cultured at 37 ^oC and 5% CO_2 in complete ReNcell® NSC Maintenance medium (EMD Millipore) supplemented with 20 ng/mL of bFGF (basic Fibroblast Growth Factor) and EGF (Epidermal Growth Factor) (EMD Millipore) in matrigel (Corning) coated tissue culture flasks.

7.2 Lentivirus and HIV-NLAD8 virus generation

The lentivirus vector encoding candidate miRNAs of interest (pictured below) were purchased from GeneCopoeia. The vector is a pEZx-MR03 (HIV-based) construct which consists of the miRNA gene with an upstream eGFP reporter. This is surrounded by 5' LTR and 3' LTR/poly A sequences. The plasmid also contains a puromycin resistance gene under the control of a CMV promoter which would aid in antibiotic selection experiments.

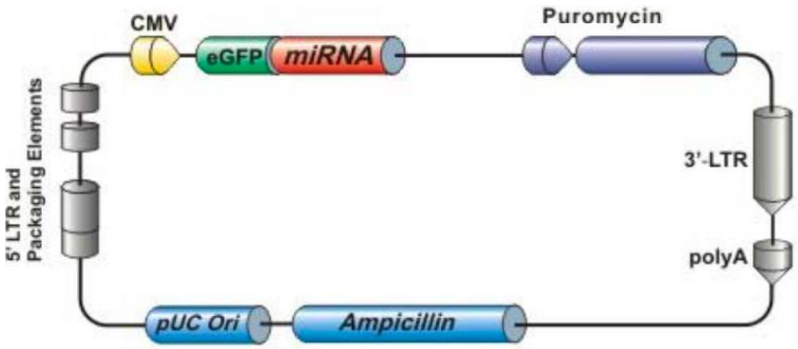

Figure 6: Schematic of miRNA-expression vector

For generating lentiviruses, HEK-293T cells were seeded at 1 x 10^6 cells in a 10 cm^2 dish and were grown to confluency overnight. Prior to transfection, the cells were replenished with fresh D10 media. For transfection, 2.75 µg of miRNA expression vector was mixed with 1.0 µg and 0.5 µg each of packaging plasmids PLP1 and PLP2 (which provide *gag*/*pol* and *rev* genes, respectively) and 0.5 µg of VSV-G plasmid encoding the vesicular stomatitis virus G glycoprotein with 250 µL of plain DMEM medium. Simultaneously, 15 µL of PolyJet™ In vitro DNA Transfection Reagent (SignaGen Laboratories) was mixed with 250 µL of plain DMEM and added to the plasmid mixtures. After incubation for no more than 20 mins, the plasmid-PolyJet™ mixture was added dropwise to the HEK-293T cells. The transfected cells were replaced with fresh D10 media after overnight incubation. 48 hours post-transfection, conditioned media from the cells were harvested by centrifuging at 1000 rpm for 5 minutes. Lentiviruses were further concentrated by centrifuging at 20,000 rpm for 1 hour.

For infectious virus generation, HEK-293T cells were seeded at 1 x 10^6 cells in a 10 cm^2 dish and were grown to confluency overnight. Prior to transfection, the cells were replenished with fresh D10 media. For transfection, 3.5 µg of $HIV_{NLAD8\text{-}DsRed}$ and 1.5 µg of VSV-G plasmid encoding the vesicular stomatitis virus G glycoprotein with 250 µL of plain DMEM medium.

$HIV_{NLAD8\text{-}DsRed}$ is a replication-competent macrophage (CCR5) tropic strain derivative of pNL4-3 tagged with an RFP construct. This virus construct was generated as described here (208) and was a kind gift from Dr. Terahara, Japan. Simultaneously, 15 μL of PolyJet™ In vitro DNA Transfection Reagent (SignaGen Laboratories) was mixed with 250 μL of plain DMEM and added to the plasmid mixtures. After incubation for no more than 20 mins, the plasmid-PolyJet™ mixture was added dropwise to the HEK-293T cells. The transfected cells were replaced with fresh D10 media after overnight incubation. 48 hours post-transfection, conditioned media from the cells were harvested by centrifuging at 1000 rpm for 5 minutes to remove cell debris. The supernatant was then filtered using a sterile, 0.22 μM syringe filter (Steriflip®, Millipore) and infectious viruses were concentrated by centrifuging at 20,000 rpm for 1 hour.

7.3 Virus Titration-U87MG assay

For virus titration, 5 x 10^3 U87MG $CD4^+$ $CCR5^+$ cells were seeded in a flat-bottom 96 well plate and were grown to confluency overnight. Serial dilutions of miRNA-encoding lentiviruses (1:100, 1:1000, 1:10,000 etc.) were prepared and added to the confluent U87MG cells. Fresh media was replaced 24 hours following infection and the cells were incubated for another 48 hours. Following this, no. of GFP+ (or RFP+ for infectious viruses) cells were counted, and the infectious particles/mL (IP/mL) was calculated using the following formula.

$$Infectious\ particles/mL = Average\ no.of\ fluorescent\ cells * Dilution\ factor * 5$$

7.4 Lentivirus transduction and puromycin selection

Approximately, 7 x 10^4 immortalized HMC3 microglial cells were seeded in a 24-well plate and were grown to confluency overnight. After replenishing the cells with fresh media, lentiviruses encoding candidate miRNAs of interest were added to the HMC3 cells at an MOI of 1 and incubated overnight. The cells were then split into 8 wells (x4 duplicates) and allowed to adhere overnight. A puromycin kill-curve experiment was conducted using multiple concentrations of puromycin (0.25, 0.15, 0.1, 0.05 and 0.01 μg/mL) (Gibco™) to identify the optimal antibiotic dose for successful selection of stably transduced microglia. The optimal antibiotic concentration is the lowest antibiotic concentration at which all cells are dead after 1 week. Using this optimal concentration, stably transduced HMC3 microglia were generated and expanded. Cell stocks were also cryopreserved in D10 containing 10% DMSO (Sigma-Aldrich) for further experimental use.

7.5 ReN cell differentiation and organoid generation

For 2D culture, approximately 3 x 10^5 ReN cells were seeded in a 6-well plate and were grown to confluency overnight. The following day, the cells were replenished with ReN differentiation medium (ReN maintenance medium + (1% FBS or GDNF or both)) and allowed to differentiate for three weeks. After 3 weeks, cultures were lysed and whole-cell RNA was isolated.

For 3D culture, approximately 7 x 10^4 ReN cells were seeded into each well of a U-bottom 96-well plate (Nucleon™ Sphera™ Thermo Scientific) allowed to congregate into neurospheres overnight. Meanwhile, parafilm strips were sterilized by UV-irradiation on which neurospheres are placed. After draining excess media, 15 μL of Matrigel (Corning) was added to the

neurospheres. These matrigel-encapsulated neurospheres were incubated at 37 ^{o}C for ~20 mins. Following the required incubation, the neurospheres were flushed off from the parafilm with complete ReN medium onto a low-attached 10 cm^2 cell culture and incubated at 37 ^{o}C. The following day, the organoids were replaced with ReN maintenance medium with 1% FBS and incubated at 37 ^{o}C for three weeks with constant rocking to prevent adherence to the plate.

7.6 RNA isolation and real-time quantitative PCR of ReN cells and 3D organoids

For RT-PCR reactions, whole cells RNA was isolated using mirVana^{TM} RNA isolation kit (Ambicon, Life Technologies) as per the manufacturer's instructions. Briefly, >1 x 10^5 ReN cells or ~10 organoids were lysed with 600 µL of RNA lysis buffer and homogenized with a p1000 pipette. Then, equal volumes of Acid-Phenol:Chloroform mixture was added and centrifuged at 13,000 rpm for 5 mins to separate the aqueous and organic phase. The upper aqueous layer is then carefully removed and transferred to another microcentrifuge tube, to which 1.25 volumes of 100% ethanol was added and vortexed thoroughly. 700 µL of this solution was transferred at a time to a supplied filter cartridge (with a collection tube) and centrifuged at maximum speed for 15 seconds to discard the flow-through. This was repeated until the entire volume of ethanol mixture was processed. To the filter cartridge, 700 µL of Wash Buffer 1 was added and centrifuged for 15 seconds. The flow-through was discarded and 500 µL of Wash Buffer 2/3 was added to the same tube and centrifuged for 15 seconds. After removing the flow-through, 500 µL of Wash Buffer 2/3 was added again and the tube was centrifuged at 13,000 rpm for 1 minute to completely dry the cartridge. The dried cartridge was then transferred to a new collection tube to which 10-50 µL of Elution Buffer was added. The tube was then centrifuged at 13,000 rpm for 20-30 seconds to elute

RNA. The purity and quantity of the RNA were calculated using NanoDrop™ 2000 spectrophotometer (Thermo Scientific). Eluate with an A260/A280 ratio between 1.9-2.1 was regarded as highly pure RNA which was then used for further downstream qPCR. To quantify neuronal and astrocytic markers, the qPCR reaction carried out in a two-step fashion: reverse transcription (to generate cDNA) and TaqMan Real-Time PCR. The reaction specifics for both the steps are as follows. Following PCR, fold change was calculated using $2^{\wedge\Delta\Delta Ct}$ method and normalized using RPLP0 as the endogenous control.

Table 2: cDNA conversion reaction-reagent specifications

Reagent	*Volume*	*Quantity/Concentration*
RT Buffer	2 µL	10x
dNTP Mix	0.8 µL	25x
RT Random Primer	2 µL	10x
Multiscribe Reverse Transcriptase	1 µL	-
RNA	Variable	10 ng/µL
Nuclease free water	Variable	-
Total	20 µL	

Table 3: Real-time qPCR reaction-reagent specifications

Reagent	*Volume*
TaqMan Master Mix	10 µL
TaqMan Assay Probes	1.75 µL
cDNA	6 µL
Nuclease free water	Up to 35 µL
Total	10 µL (x3 triplicates)

7.7 Genomic DNA isolation and polymerase chain reaction

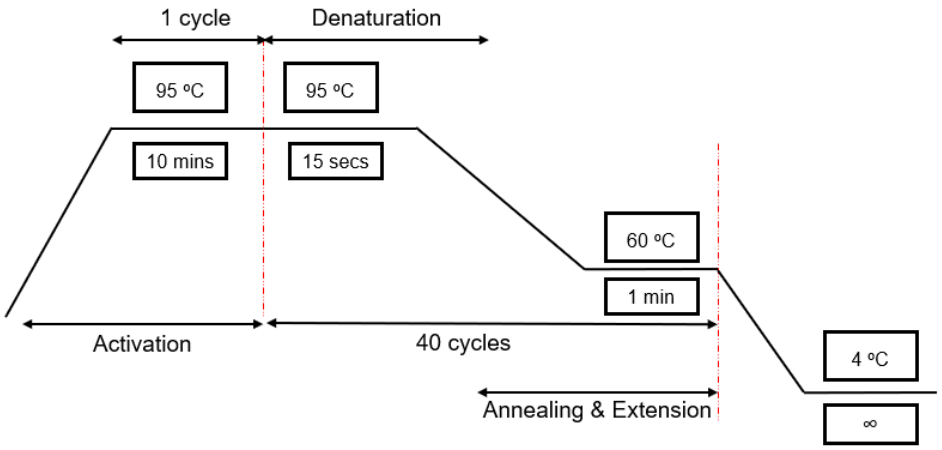

Figure 6: Schematic of PCR running conditions

Genomic DNA (gDNA) from transduced and untransduced microglia were isolated using All Prep DNA/RNA Mini Kit (Qiagen) according to the manufacturer's instructions. Briefly, 5 x 10^5 cells were lysed with 350 µL of Buffer RLT Plus and the lysate was homogenized with a p1000 pipette. The homogenized lysate was transferred to an All Prep DNA spin column and centrifuged at ≥10,000 rpm for 30 seconds. The spin column was transferred to a new collection tube and 500 µL of Buffer AW1 and spun at 10,000 rpm for 15 seconds. The flow-through was discarded and 500 µL of Buffer AW2 was added to the spin column and was centrifuged at maximum speed for 2 minutes to completely dry the column. Next, 30-50 µL of Buffer EB (preheated to 70 ºC) was added to the spin column and incubated at room temperature for 2 mins. The column was then centrifuged at 10,000 rpm for 1 minute to elute DNA. The purity and quantity of the gDNA were calculated using NanoDrop™ 2000 spectrophotometer (Thermo Scientific). The resulting gDNA was then amplified through conventional PCR using SYBER™ Select Master Mix with appropriate primers. The PCR products were then visualized through gel electrophoresis on 2%

agarose (Seakem® LE Agarose, Lonza Biosciences) at a constant voltage of 90V with a 100 bp ladder (Gene ruler 100bp, Thermo Scientific) for comparison.

Table 4: gDNA PCR-reagent specifications

Reagent		*Volume*	*Quantity/Concentration*
SYBER™ Select Master Mix		10 µL	-
Primers	Forward	1.2 µL	10 µM
	Reverse	1.2 µL	10 µM
gDNA		Variable	0.1-0.2 µg
Nuclease free water		Variable	-
Total		20 µL	

7.8 Fluorescence microscopy and flow cytometry

Approximately, 1 x 10^5 cells were seeded in a 24-well plate with a sterile coverslip and were grown to confluency overnight. Adherent cells were washed twice with sterile 1x PBS (Corning®) and fixed with 4% paraformaldehyde solution for 20 minutes. Fixed cells were washed twice again with PBS and stained with DAPI for 1-2 minutes. Stained cells were washed once more with PBS and the coverslips were aseptically removed and transferred to a clean glass slide with 90% glycerol mounting medium and were allowed to dry overnight. Dried coverslips were then visualized using Nikon E1000 Epifluorescence microscope and edited using ImageJ.

For flow cytometry, a similar amount of cells was seeded and allowed to adhere overnight. Adherent cells were then dispersed with minimal trypsin into single-cell suspensions and transferred to a sterile V-bottom 96 well plate. The plate was centrifuged in a microplate compatible centrifuge at 2500 rpm for 5 minutes. The pelleted cells were then stained for viability using LIVE/DEAD™ Aqua Dead Cell Stain Kit (Invitrogen™) at a working dilution of 1:500 for

30 minutes. Following this, the cells were pelleted by centrifuging at 2500 rpm for 5 minutes and fixed in 4% paraformaldehyde. Flow cytometry and subsequent analysis of the fixed cells was done using LSRFortessa^{TM} (BD Biosciences) and FlowJo v.10.7.1, respectively.

7.9 HIV infection and cytokine ELISA

Approximately, 1 x 10^5 cells were seeded in a 24-well plate and allowed to grow to confluency overnight. Adherent cells were replenished with fresh media and infected with HIV-1 (MOI of 1 and 0.5) or mock-infected with equal quantities of sterile PBS. Conditioned media was harvested from treated cells at 18 & 48 hours and cytokine concentrations were quantified through DuoSet Human TNF-α/IL-1β ELISA kit (R&D Biosystems) according to manufacturer's instructions.

Briefly, a sterile 96-well was coated with 100 µL of the working dilution of the primary capture antibody in PBS (without carrier protein) overnight at room temperature. Coated plates were washed thrice with 1x PBS/0.5% Tween-20 (Fischer Scientific) and blotted dry with paper towels. The plates were then blocked with 100 µL of blocking buffer (PBS/1% BSA (Sigma)) for a minimum of 1 hour and washed thoroughly. Harvested supernatants were diluted to appropriate working dilutions and 100 µL of each was added to corresponding wells. Simultaneously, 8-point two-fold serial dilutions (1000 pg/mL to 3.61 pg/mL) of the standards were made and equal volumes were added to each well. All the samples and standards were incubated at room temperature for 2 hours. Following this, the plates were washed thoroughly three times and 100 µL of the working dilution of the secondary detection antibody (in blocking buffer) was added

with incubation at room temperature for 2 hours. The plates were washed thoroughly again and 100 µL of the working dilution of Streptavidin conjugated with HRP (Horseradish peroxidase) was added and incubated in the dark for 20 minutes. The plates were washed thrice again and 100 µL of SUREBLUE^{TM} TMB-1 (Tetramethylbenzidine) Substrate (Seracare Life Sciences Inc.) was added and incubated in the dark for 20 minutes. After 20 minutes, the reaction was stopped using 50 µL of 1 N H_2SO_4 and the plate was tapped gently to ensure complete mixing. The optical density was determined using an ELX800 Microplate Reader and KcJunior software (BioTek Instruments) set to an absorption maximum of 450 nm. Cytokine concentrations in the samples were calculated from the linear trend line equation ($R^2 \geq 0.900$) of the plotted standard curve.

Table 5: Working dilutions of ELISA reagents

Reagent		***Working Dilution/Concentration***
Primary Capture Antibody		4 µg/mL
Secondary Detection Antibody	Human anti-TNF-α	50 ng/mL
	Human anti-IL-1β	200 ng/mL
Streptavidin-HRP		1:40

7.10 Inflammasome activation and MTT assay

Approximately, 1 x 10^5 cells were seeded in a 24-well plate and allowed to grow to confluency overnight. Adherent cells were replenished with fresh media and primed with 100 ng/mL and 500 ng/mL bacterial lipopolysaccharide (Millipore Sigma) for 24 hours. Following this, the media was supplemented with 5 mM ATP (Sigma Aldrich) and conditioned media was isolated after 30 minutes. IL-1β was quantified through cytokine ELISA as mentioned in section 6.6.

For assessing cell viability, an MTT assay was performed. MTT assay is a colorimetric assay that depends on the ability of cellular NAD(P)H oxidoreductases to reduce the MTT [3-(4,5-dimethylthiazol-2-yl)-2,5-diphenyltetrazolium bromide] dye into insoluble formazan crystals. These crystals are further dissolved using a detergent solvent like DMSO, acidified isopropanol etc. and absorbance is read at specific wavelengths. This absorbance is directly proportional to the percentage of viable cells. To perform the assay, approximately 1 x 10^4 cells were seeded into a 96-well plate and allowed to grow to confluency overnight. Inflammasome activation was performed as mentioned earlier and conditioned media was discarded carefully at the end of ATP stimulation. To the cells, 90 µL of serum-free DMEM (with 1% Glutamine and Penicillin/Streptomycin, without phenol-red) and 10 µL of MTT reagent (Tocris Biosciences™) were added and the plate was incubated for 4 hours at 37 ^{o}C until purple formazan crystals are visible. After incubation, the MTT reagent was aspirated carefully and 100 µL of DMSO was added. The plate was left in an orbital shaker for 15 minutes to thoroughly dissolve the crystals. The absorbance was read at 570 nm (with a reference wavelength of 650 nm) and cell viability was calculated.

7.11 Figures and Statistical analysis

All illustrative graphics (Section 2.0-4.0) were generated through BioRender.com. Rest of the graphical and statistical summaries were performed using GraphPad Prism 8 software. Sample means were compared through a Student's *t*-test with a significance level of 0.05.

8.0 RESULTS

8.1 Aim 1: Generation of stably transduced HMC3 microglia using candidate miRNAs of interest and 3D brain organoids using immortalized human neuroprogenitor cells

To generate stably transduced microglia, lentiviral vectors encoding candidate miRNAs (miR-20a, miR-106b etc.) needed to be produced. For this purpose, Human embryonic kidney 293T (HEK 293T) cells were transfected with the miRNA expression vector and packaging plasmids containing *gag*/*rev* and VSV-G envelope plasmid. *Rev* is a transactivating protein necessary for viral RNA export and packaging. VSV-G plasmid is used to pseudotype the nascent lentiviral vectors for efficient entry into microglia.

The lentivirus titers generated through transfection (Table 6) were greatest for the two miRNAs-miR-20a and miR-106b. For scramble and miR-141, titers were low and multiple batches needed to be combined to have sufficient viruses for transduction. Following virus generation, human immortalized HMC3 microglia were transduced with the lentiviruses at an MOI of 1. Transduced microglia needed to be selected to obtain a homogenous population of miR-microglia. To do so, puromycin (an aminonucleoside antibiotic) was used. As indicated in Fig. 6, the miRNA plasmids contain a puromycin resistance gene encoding a puromycin *N*-acetyltransferase gene which inactivates the antibiotic, conferring resistance. Thus, a puromycin kill-curve experiment was conducted to determine optimal antibiotic concentrations. Of all the doses tested, 0.10 μg/mL and 0.05 μg/mL was efficient at killing untransduced cells and thus led to the generation of stably transduced microglia.

For 3D organoids, human immortalized neuroprogenitor (ReN) cells were cultured and neurospheres were generated as described before (see Materials and Methods), In a state of physiological homeostasis, the neuron-to-astrocyte ratio is estimated to be around 1:4 (209). Thus, any study attempting to extrapolate results from *in vitro* experiments requires the maximum physiological relevance possible. Therefore, before attempting 3D organoid cultures, 2D cultures of ReN cells were tested for multiple differentiation stimuli to push astrocyte differentiation. Out of the different stimuli tested, 1% FBS resulted in increased astrocyte differentiation (as evidenced by astrocytic markers, GFAP and S100β) in both 2D cultures and subsequently, 3D organoids.

8.1.1 Lentivirus production and generation of miR-microglia

To generate HMC3 microglia constitutively expressing our miRNAs of interest, lentivirus vectors were used. For this, HEK 293T cells were transfected with appropriate plasmids (as outlined before, see materials and methods) and viruses were harvested at days 72 and 96 hours post-transfection. Harvested supernatants were concentrated to improve yield and the resulting lentiviruses were titered through a U87MG assay. We initially started out with 6 candidate miRNAs and generated lentiviruses for all of them. However, virus titers were remarkably different between each of them, with miR-20a and miR-106b having the highest titers while the rest of them miRNAs produced consistently low titers. Therefore, further transduction experiments were carried out for the two miRNAs. The next step in generating stable miR-microglia was performing a puromycin kill curve experiment to select transduced cells and kill untransduced cells which will give rise to a completely homogenous cell population. The plate setup of the experiment is shown below (Figure 7); of the different concentrations of puromycin tested, 0.25

µg/mL proved to be lethal (which killed all cells by 72 hours). 0.10 and 0.05 µg/mL puromycin was effective and thus used to select and expand our miR-microglia.

Table 6: Generation and titration of miRNA lentiviruses

Experiment no.	*Lentivirus particles/mL*10^6*				
	Scramble	*miR-20a*	*miR-106b*	*miR-141*	*miR-let-7a*
TR001	0.10	2.8	0.04	0.012	0.06
TR002	0.13	1.25	0.55	0.09	0.03
TR003	0.04	0.115	0.035	0.038	0.027
TR004	0.063	-	0.11	0.035	0.028
TR005	0.03	-	-	0.09	-

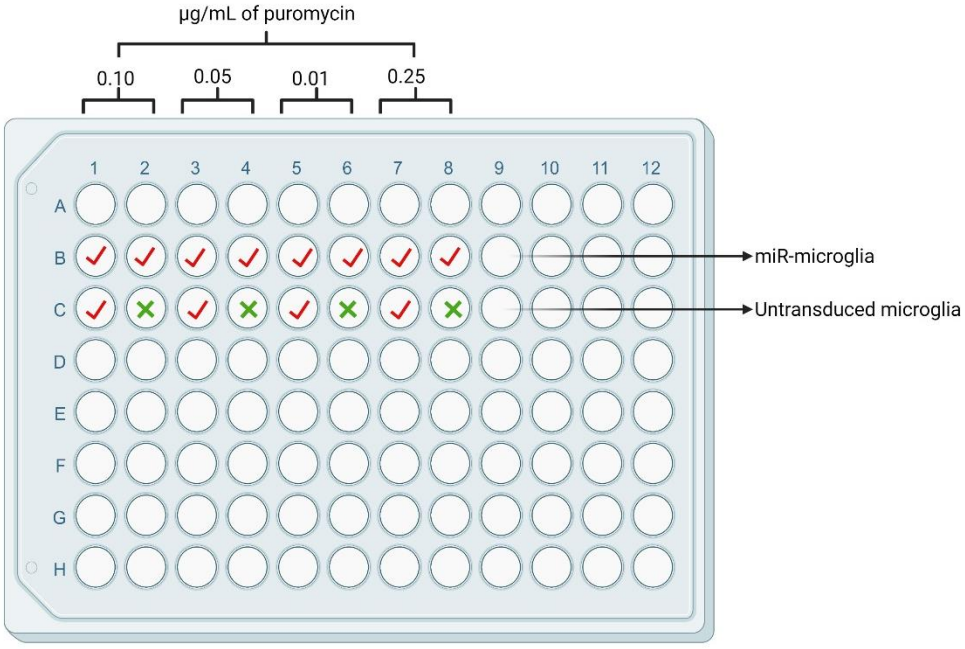

Figure 7: Plate setup of puromycin kill-curve experiment: Transduced and untransduced HMC3 cells were seeded in duplicates. After cell attachment, puromycin was added (red check) and one well was left as a non-antibiotic control (green cross).

a)

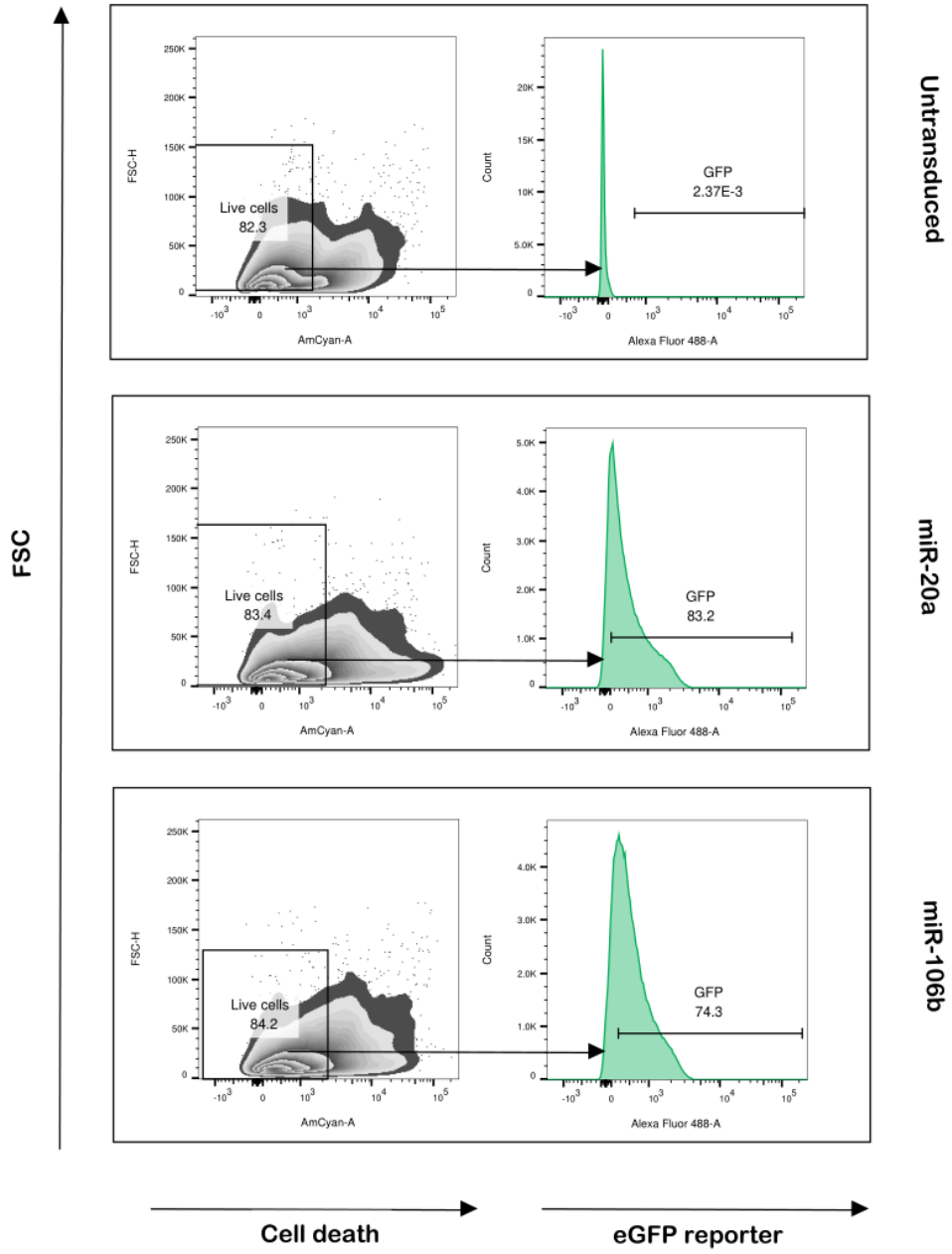

Figure 8: Transduction efficiency of miRNA-expressing HMC3 microglia: HMC3 microglia were transduced at an MOI (multiplicity of infection) of 1 and subjected to 0.10-0.2 µg/mL puromycin until the successful selection was achieved. Transduced cells were stained with Aqua LIVE/DEAD™ viability stain and visualized through flow cytometry.

b)

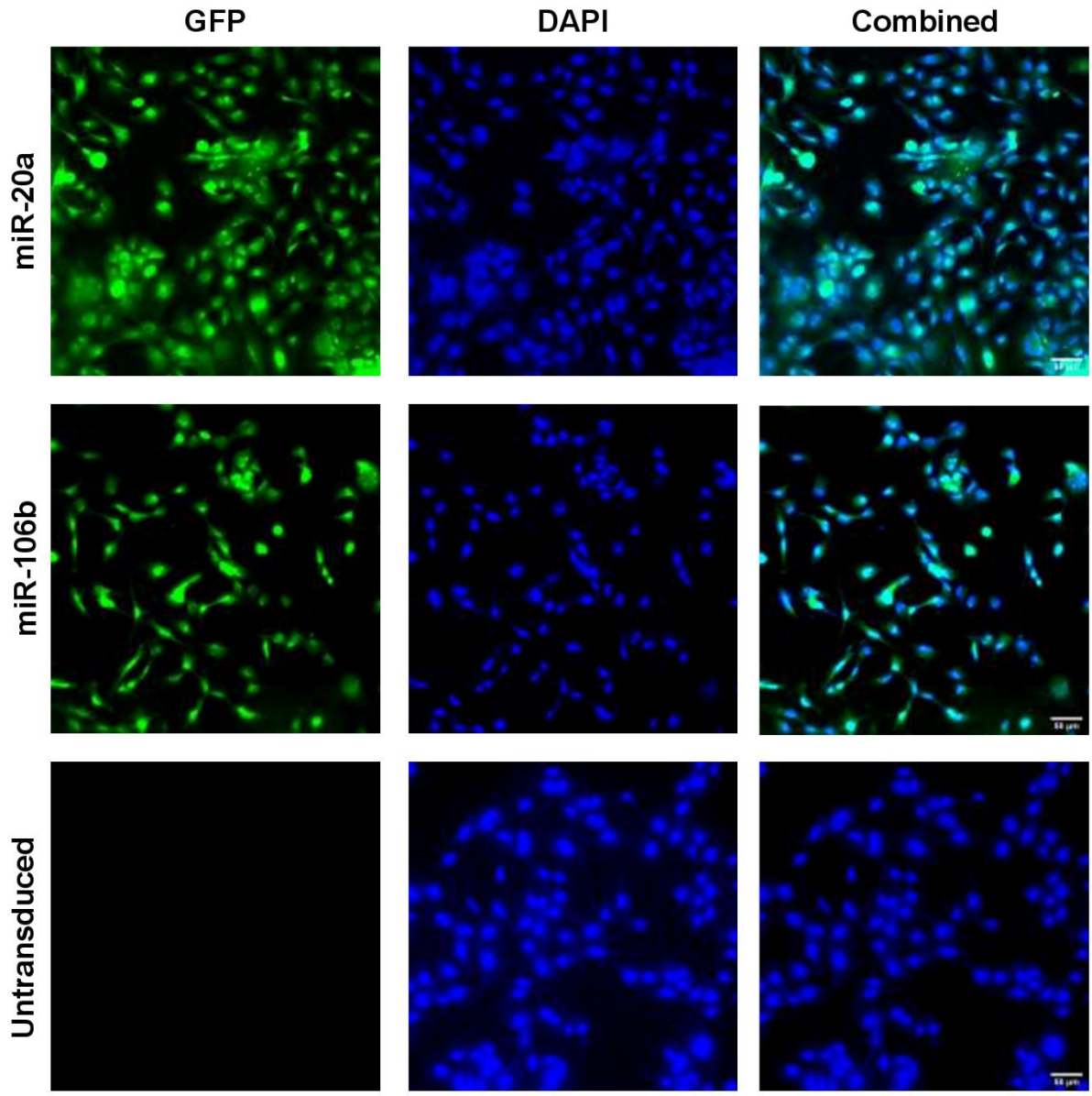

Figure 9: Transduction efficiency of miRNA-expressing HMC3 microglia: HMC3 microglia were transduced at an MOI (multiplicity of infection) of 1 and subjected to 0.10-0.2 μg/mL puromycin until the successful selection was achieved. Transduced cells were stained with DAPI and visualized through fluorescence microscopy. Scale bar indicates 50 μm.

From Figure 8, it can be seen that nearly all of the HMC3 microglia in the treatment groups had >90% transduction efficiency (as suggested by GFP expression). Even after 30 passages, these miR-microglia were observed to have similar reporter expression (image not shown) indicating successful stable transduction.

8.1.2 Validation of miR-microglia

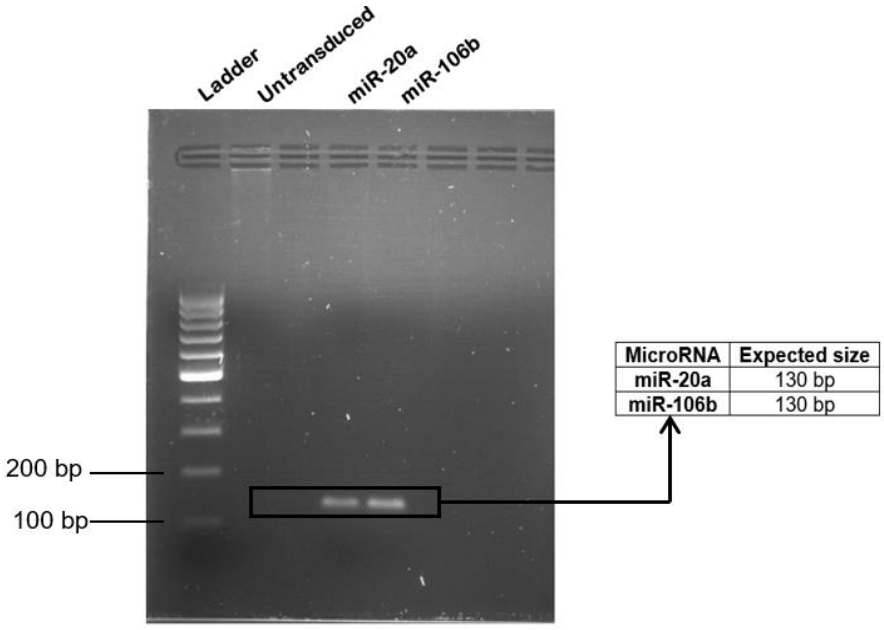

Figure 10: Validation of miR-microglia through genomic PCR: Genomic DNA was isolated and PCR reaction was performed as mentioned earlier. The products were run undigested on a 2% agarose gel.

Though eGFP reporter expression serves as an indirect marker of transduction, successful genomic insertion of the lentiviral vector needed to be confirmed. When the genomic PCR products were resolved on an agarose gel, miR-20a and miR-106b expressing microglia had a distinct band at the anticipated size (130 bp) while the untransduced control did not have a band. This indicates successful insertion of our miRNA construct into the microglial genome.

8.1.3 Generation of 3D brain organoids

Human immortalized neuroprogenitor cells a.k.a ReN cells are multipotent stem cells capable of differentiating into multiple cells of the neuroepidermis namely, neurons, astrocytes etc. Under *in vitro* culture conditions, ReN cells are maintained in their multipotent state by bFGF and EGF growth factor supplements in their culture media which arrest their differentiation into neurons and astrocytes. When the neural supplements are removed, ReN cells spontaneously begin their differentiation. However, differentiating ReN cells give rise to an abundance of cells of neuronal lineage and less of glial cells like astrocytes. However, under conditions of physiological homeostasis, the total percentage of astrocytes in the CNS niche is 3-4 times greater than that of neurons (209). Thus, in order to achieve greater physiological relevance, ReN cell cultures were subjected to multiple differentiation stimuli and their effect on subsequent differentiation to astrocytes was assayed through reverse transcriptase-qPCR (RT-PCR). Of the three tested stimuli (1% FBS or GDNF or 1% FBS+GDNF), ReN cell medium containing 1% FBS was found to be effective at driving astrocyte differentiation as indicated by the increased expression of its corresponding markers: GFAP and S100β (Figure 10a). Following this, 3D brain organoids were produced as outlined in section 7.5 and grown in ReN medium containing 1% FBS. Three-week old organoids (Figure 10c) were then lysed and whole cell RNA was then isolated using which RT-PCR was performed. Similar to the 2D culture, 1% FBS resulted in a higher proportion of astrocytes than neurons as inferred from the expression level of their respective markers, GFAP and Tubulin (Figure 10b).

a)

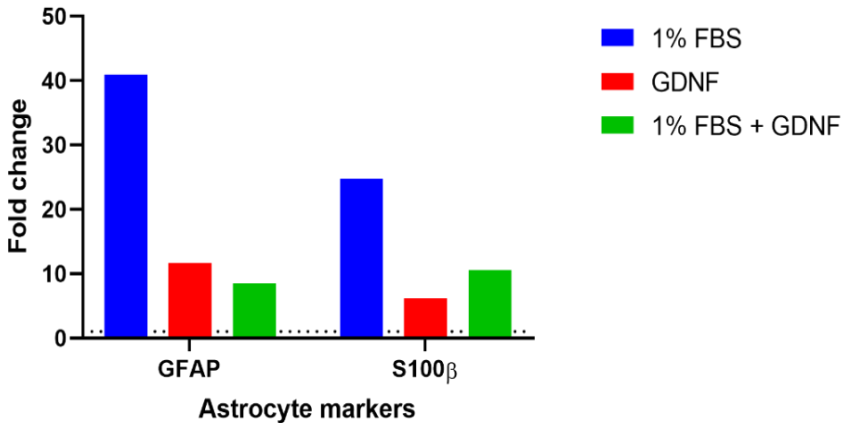

b)

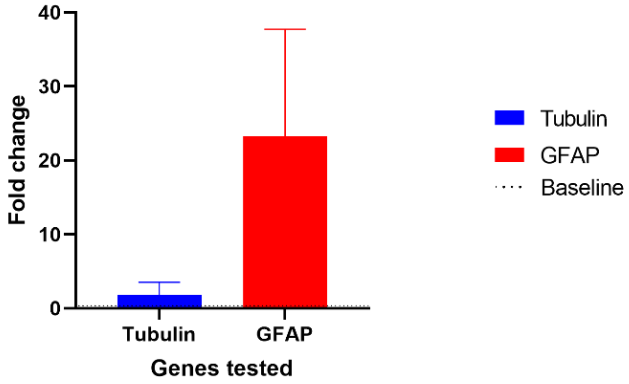

c)

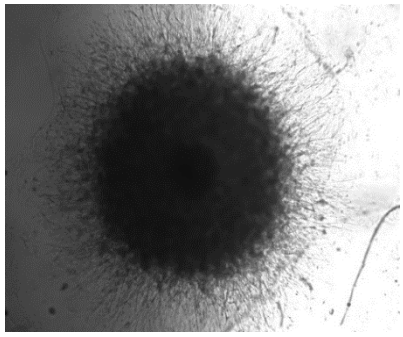

Figure 11: ReN cell differentiation in 2D culture (a) and 3D organoid culture (b & c): Human immortalized neuroprogenitor cells were cultured as mentioned earlier. Following differentiation, both the cultures were lysed and whole-cell RNA was extracted. Neuronal and astrocytic markers were amplified through RT-qPCR and gene expression was normalized using Ribosomal Protein Lateral Stalk Protein Subunit (RPLP0). A representative phase-contrast image of a three-week-old organoid is shown in (c) (n=1).

8.2 Aim 2: Investigate the anti-inflammatory effects of candidate miRNAs and their subsequent role in preventing HIV-1 replication and HIV-mediated inflammation.

Once stable miR-microglia were generated, the supposed anti-inflammatory effects of the candidate miRNAs needed to be tested. To do so, both transduced and untransduced HMC3 microglia were either stimulated with multiple concentrations of bacterial lipopolysaccharide(LPS)/poly I:C, LPS/ATP or infected with infectious HIV-$1_{NLAD8\text{-}DsRed}$ virus at varying MOIs for defined time points. Following this, the inflammatory response to these stimuli was quantified through an ELISA.

In addition to evaluating the anti-inflammatory effects of miRNAs, we were interested to investigate the possibility that these miRNAs might modulate virus replication, either positively or negatively. For instance, miR-122 is notorious for its indispensable role in aiding HCV replication and has therefore stemmed FDA-approved therapeutics like Miravirsen for treating chronic HCV (210). Thus, it was imperative for this study to focus on the effect of miR-microglia on HIV-1 replication as well.

For investigating the anti-inflammatory effects of over-expressing candidate miRNAs, miR-microglia were either stimulated with LPS (1.5 μg/mL), Poly I:C (20 μg/mL), LPS (500 ng/mL & 100 ng/mL)→ATP (5 mM) or infected with HIV-$1_{NLAD8\text{-}DsRed}$ virus at an MOI of 1 and 0.5. Following this, conditioned media was harvest at 0, 24, 48 and 72 hours (for LPS and Poly I:C), 0, 24 hours (for LPS→ATP) and 0,18,48,72 hours (for HIV-1 infection). Cytokines in the conditioned media were then quantified through ELISA.

8.2.1 Effect of miR-microglia on sterile inflammation

Initially, to test the response of untransduced and transduced microglia to sterile inflammatory stimuli, bacterial lipopolysaccharide (1.0, 1.5 µg/mL) and Poly I:C (20 µg/mL) were used as TLR stimulants. However, both stimuli failed to elicit a strong enough response (data not shown) which was in accordance with previously published results on HMC3 microglia (211). Therefore, the response of microglia to inflammasome activation was tested instead and a similar experimental plan as detailed in Hu Li. Et al was followed (212). Following LPS priming and ATP activation, IL-1β secretion was quantified through an ELISA and pyroptosis (a form of inflammatory cell death) was quantified through an MTT assay.

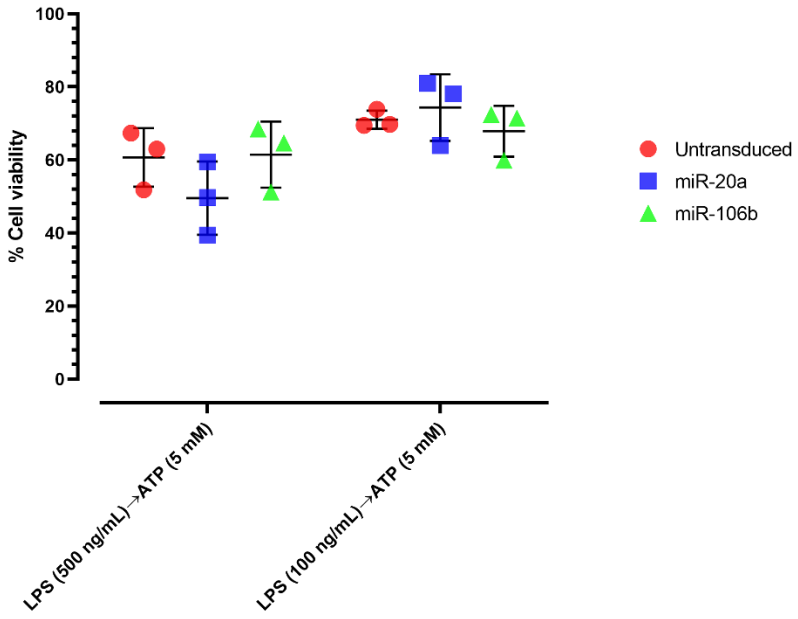

Figure 12: Cell viability following pyroptosis: Transduced and untransduced microglia were primed with indicated concentrations of LPS for 24 hours and activated with 5mM ATP for 30 minutes. Following this, the viability of cells was tested through an MTT assay and compared with their unstimulated counterparts (n=1).

Similar to the TLR stimulation experiments, LPS/ATP stimulation failed to elicit a strong, quantifiable IL-1β response (data not shown). Interestingly, cells did respond with changes to their overall morphology following ATP addition, which indicates that 30 minutes might not be sufficient time for detectable levels of IL-1β to accumulate in the conditioned media. The viability of cells followed inflammasome activation was measured through an MTT assay (see Materials and Methods) and % cell viability was calculated as follows:

$$\%\ cell\ viability_{treatment} = \frac{Corrected\ OD_{treatment}}{Corrected\ OD_{control}} * 100$$

Note: corrected OD was calculated by subtracting the individual OD values with the blank OD of DMSO control.

At both doses of LPS (500 and 100 ng/mL), there was a decrease in overall viability as opposed to their unstimulated controls. However, no significant difference in cell survival was observed between transduced and untransduced microglia (Figure 11).

8.2.2 Effect of miR-microglia on HIV-1 mediated inflammation

Following TLR activation experiments, the anti-inflammatory effects of miR-microglia in the context of HIV-1 infection needed to be investigated. For this, transduced and untransduced microglia were infected with HIV-$1_{NLAD8\text{-}DsRed}$ virus at an MOI of 1 and 0.5. Following infection, conditioned media was isolated from cells at 18, 48 and 72 hours post-infection and levels of TNF-α/IL-1β were quantified through cytokine ELISA (Figures 12 and 13).

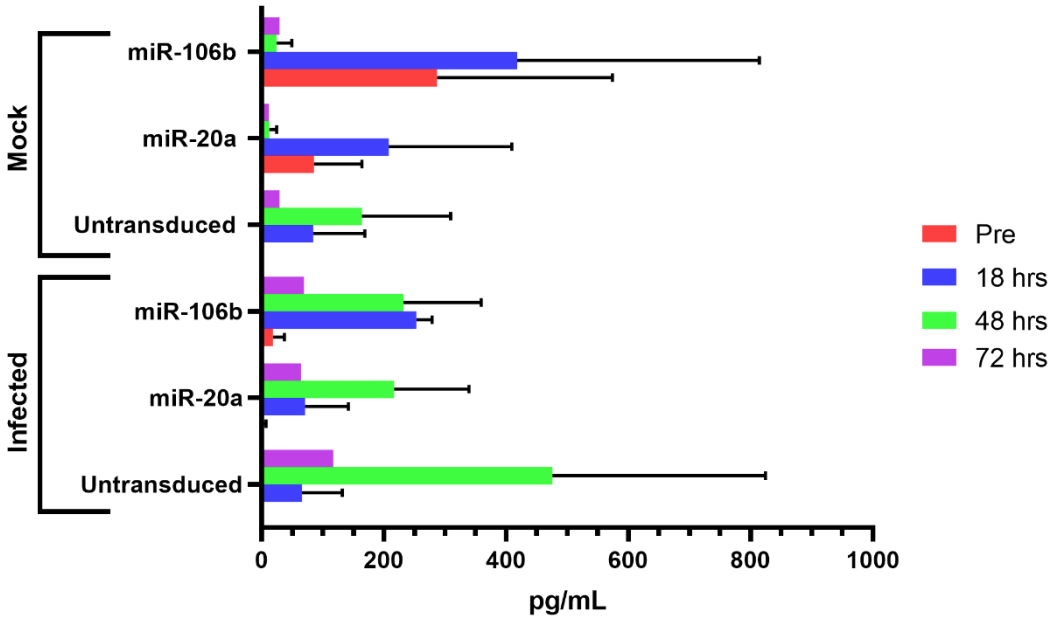

Figure 13: TNF- α expression following HIV-1 infection of HMC3 microglia: Transduced and untransduced were infected with HIV-NLAD8 at a multiplicity of infection (MOI) of 1. Conditioned media was isolated at indicated times and TNF-α in the supernatants was quantified by ELISA (n=2).

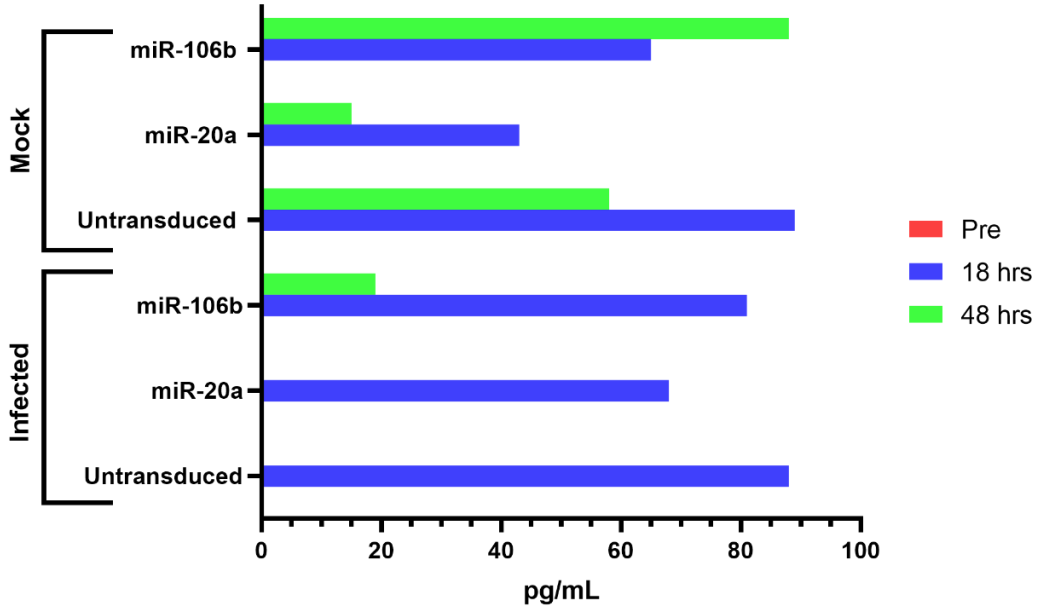

Figure 14: IL-1β expression following HIV-1 infection of HMC3 microglia: Transduced and untransduced were infected with HIV-NLAD8 at a multiplicity of infection (MOI) of 1 and 0.5. Conditioned media was isolated at indicated times and IL-1β in the supernatants was quantified by ELISA (n=1).

Untransduced microglia had a robust TNF-α response at about 48 hours post infection. This was matched by a much smaller release of TNF-α in both miR-20a and miR-106b expressing microglia, suggesting an anti-inflammatory effect of these miRNAs. All of these responses, however, reached similar levels at 72 hours post infection (Figure 12). On the contrary, both transduced and untransduced microglia displayed a weaker IL-1β response and no significant difference between the microglia was observed (Figure 13).

8.2.3 Effect of miR-microglia on HIV-1 infection and replication

In an attempt to examine the effect of our candidate miRNAs on HIV-1 replication, transduced and untransduced microglia were infected with HIV-$1_{NLAD8\text{-}DsRed}$ virus at an MOI of 0.5 and 0.1. Following infection, the cells were monitored for RFP expression which occurred roughly around 48-72 hours post-infection. For virus titer assays, conditioned media was isolated at 48 and 72 hours post-infection and 100 μL of undiluted supernatant was added to U87MG cells for quantifying infectious particles. On the contrary, for flow cytometry, infected cells 72 h.p.i were stained for viability and fixed with 4% paraformaldehyde. Fixed cells were then visualized using flow cytometry and gated on PE-C594-A channel to quantify HIV-1 infection. Upon analysis, both miR-microglia and untransduced HMC3 microglia did not have any significant differences in the total percentage of HIV-1 infected cells (Figure 14b). This means that the overexpression of miR-20a and miR-106b did not affect the ability of HIV-1 to infect these microglia. Subsequently, the relative median fluorescence intensity (RMFI) was also calculated for the same channel from the median fluorescence intensities (MFIs) of infected and uninfected microglia (Figure 14c).

a)

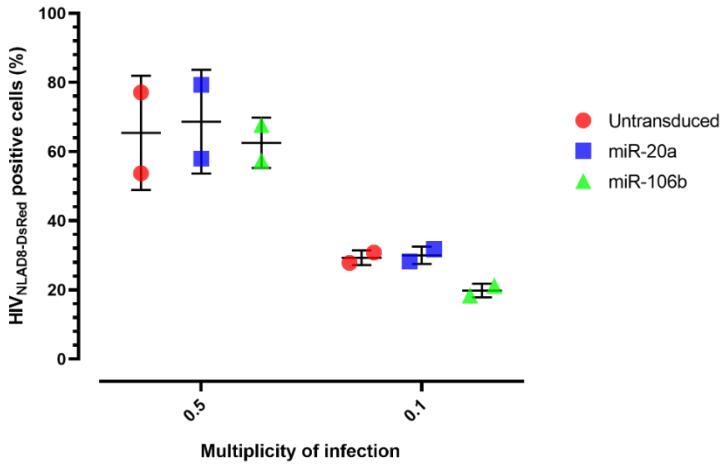

b)

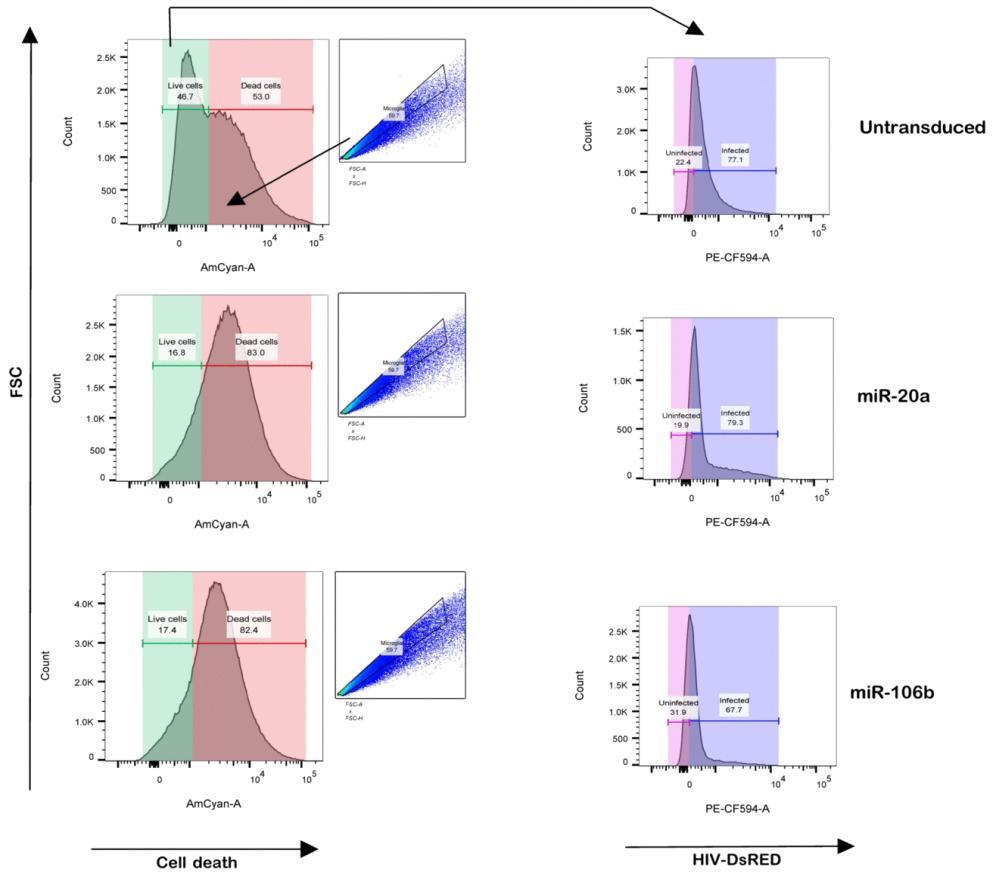

Figure 15: Flow cytometry of HIV-1 infected HMC3 microglia: Transduced and untransduced microglia were either infected with HIV-$1_{NLAD8\text{-}DsRed}$ at MOI of 0.5 and 0.1 or mock-infected with sterile PBS. Cells were harvested at 72 h.p.i and Flow cytometry was done using BD Fortessa™ and subsequent analysis was done using FlowJo v.10.7.1. Percentage total infection (a) was calculated using the gating strategy shown in (b).

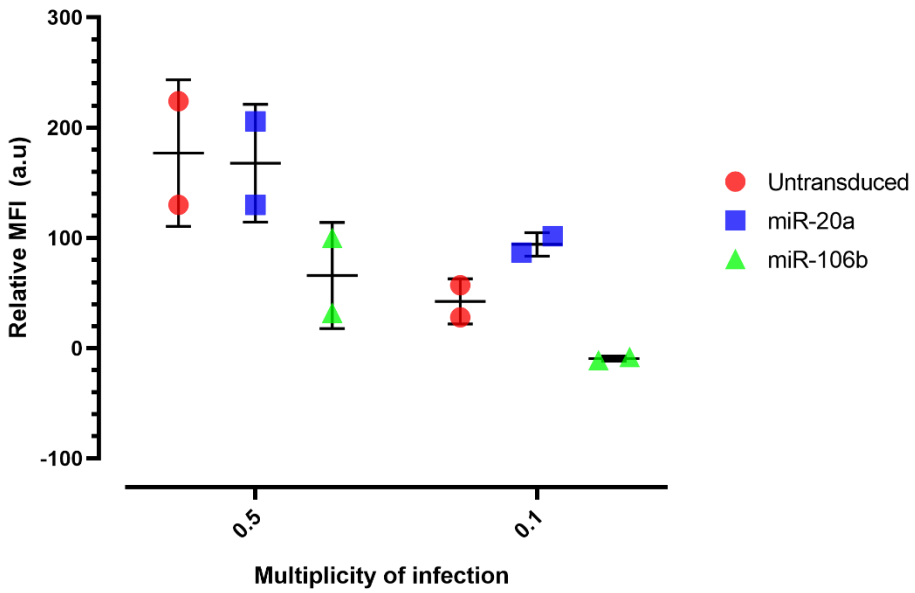

Figure 16: Flow cytometry of HIV-1 infected HMC3 microglia: Transduced and untransduced microglia were either infected with HIV-$1_{NLAD8\text{-}DsRed}$ at MOI of 0.5 and 0.1 or mock-infected with sterile PBS. Cells were harvested at 72 h.p.i and Flow cytometry was done using BD Fortessa™ and subsequent analysis was done using FlowJo v.10.7.1. Relative MFI was calculated using the formula: $MFI_{infected} - MFI_{uninfected}$ (n=2) (c).

As seen in Figure 14c, miR-106b had an overall less RMFI as opposed to both miR-20a and untransduced microglia at both the MOIs. Since RMFI represents the medium fluorescence intensity of a particular channel (after background subtraction), low RMFI of miR-106b represents an overall lower level of HIV-1 replication compared to the other two groups. To confirm this inference regarding the diminishing effect of miR-106b on HIV-1 replication, concomitant cultures with similar conditions were set up to directly analyse the virus titers following infection (Figure 15).

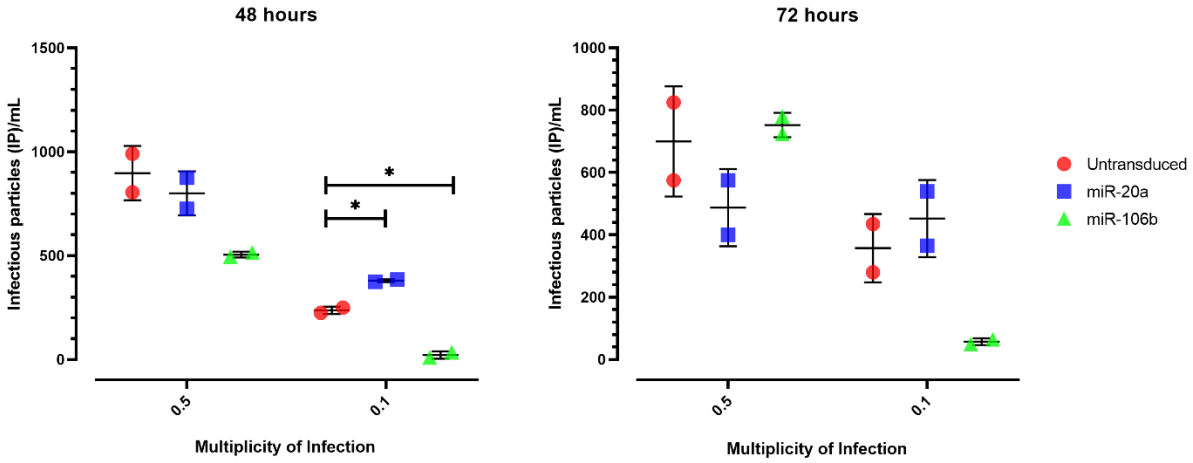

Figure 17: Virus titers in the conditioned media of HIV-1 infected HMC3 microglia: 48 hours (left) and 72 hours (right): Transduced and untransduced microglia were either infected with HIV-$1_{NLAD8\text{-}DsRed}$ at MOI of 0.5 and 0.1 or mock-infected with sterile PBS. Conditioned media was harvested at 48 and 72 h.p.i and virus titers were quantified through a U87MG assay and represented as Infectious particles(IP)/mL (n=2, *, $p<0.05$).

Similar to the results observed in Figure 14, miR-106b expressing microglia displayed significantly lower virus titers at both 48 and 72 hours post-infection at both the MOIs (Figure 15). Specifically, the titers at 48 hours/MOI 0.1 exhibited a statistically significant difference between the untransduced and miR-106b microglia. Together, these results suggest that miR-106b expressing HMC3 microglia exhibit a diminshed rate the viral replication leading to comparitively low virus titeres than untransduced and miR-20a-expressing microglia. The effect of miR-20a on HIV-1 replication appears to be inconclusive and needs more biological replicates to establish the presence or absence of a statistically significant relationship.

9.0 CONCLUSIONS AND DISCUSSION

HIV-1 infection and persistence in microglia in the early phase has been proved to be very important for the establishment of latency in the CNS of infected people (213). Besides, HIV-infected microglia have been implicated in the neurodegenerative processes associated with the development of HAND. Lastly, select candidate miRNAs were previously identified by our group to be differentially expressed in the PBMCs of HIV+ HAND+ patients. This led to our hypothesis about the potential use of these miRNAs as therapeutics to halt or treat the prognosis of HAND. Specifically, microglia overexpressing these miRNAs a.k.a miR-microglia were evaluated for their role in modulating HIV-1 infection and HIV-mediated inflammation.

For the generation of miR-microglia, lentiviruses containing the miRNA-expression vector were generated by transfection of HEK 293T cells. While miR-20a and miR-106b consistently produced high titers, other miRNAs namely, miR-141, miR-let-7a and scramble control miRNA had weak yields making stable transduction difficult. Thus, miR-20a and miR-106b were subsequently used to generate miR-microglia. However, we were still able to generate miR-141 and scramble microglia by combining and concentrating multiple transfections but these microglia were not included as part of our investigation.

For stable transduction of microglia, HMC3 cells were infected at an MOI of 1 with appropriate lentiviral constructs and selected at varying concentrations of puromycin to create a homogenous population of miR-microglia. While puromycin, in general, is toxic to mammalian cells (214), miR-microglia were observed to be resistant to low doses of the antibiotic. Hence, a puromycin kill-curve/titration experiment was conducted to determine the optimal puromycin

concentration; this was found to be 0.1 and 0.05 µg/mL. This batch of miR-microglia was further expanded, cryopreserved and used for further experiments.

Regarding 3D organoids, ReN cells were seeded at desire numbers to form neurospheres. These neurospheres were then used to generate our organoids by procedures outlined in the methods section. To establish physiological relevance, organoids should have a higher proportion of astrocytes in them than neuronal cells. Hence, multiple differentiation stimuli were tested among which organoids in ReN maintenance medium supplemented with 1% FBS had a higher differentiation of progenitor cells into astrocytes. While the initial idea was to determine the astrocyte, neuron and progenitor cell population through flow cytometry, we were hindered due to the difficulty in generating single-cell suspension. Thus, we chose to analyse the cell population using RNA markers instead of using real-time quantitative PCR.

Aim 2 of our project examined the protective (or lack thereof) role of miR-microglia in the context of both sterile and HIV-mediated inflammation. Initially, TLR stimulants like bacterial lipopolysaccharide (TLR2/4 agonist) and polyinsonic:polycytidylic acid (TL3 agonist) were used to assess their effect of miR-microglia. However, a weak to negligible response to these pro-inflammatory stimuli (as quantified by TNF-α and IL-1β levels) meant we could not draw meaningful conclusions. Following this, inflammasome activation was performed using a combination of LPS and ATP and enusing IL-1β release was quantified. Since inflammasome activation is followed by pyroptosis (215), cell viability was also assessed simultaneously through an MTT assay. Similar to previous experiments, inflammasome activation did not result in a strong response from HMC3 microglia despite showing morphological changes upon ATP addition. When cell viability was assessed, no difference in cell survival was found among the transduced and untransduced microglia.

On the contrary, both untransduced and miR-microglia had a significant TNF-α response; this response was more pronounced in untansduced microglia than miR-microglia (at 48 hours post infection). This could point to a potential anti-inflammatory effect of these miRNAs in these microglia, barring further investigation. Regarding IL-1β, a strong type 1 Interferon response had been known to surpress IL-1β release (216), which would explain the weak response seen during HIV-1 infection. Hence, future experiments analysing IFN-1 levels may be needed to explain this aberration.

Following HIV-1 infection, the percentage of infected cells was analysed through flow cytometry. This revealed that both transduced and untransduced microglia had no significant difference in the level of infection indicating that these miRNAs do not directly affect virus entry and infection. Subsequently, the RMFIs were calculated from the median intensities of infected and uninfected samples which revealed a remarkedly lower level of active HIV-1 replication in miR-106b expressing microglia as opposed to both untransduced and miR-20a expressing microglia. Similar trends were observed when total infectious viruses in the conditioned media were quantified which suggested that miR-106b might hinder the rate of virus replication in microglia.

9.1 Future Directions

While our preliminary results indicate that miR-20a and miR-106b have a mild anti-inflammatory role, there is strong evidence about the role of miR-106b in controlling HIV-1 replication in transduced HMC3 microglia. Since certain miRNAs have been known to target virus replication, further investigation on the detailed role of miR-106b in influencing HIV-1 replication

is warranted through loss-of-function studies in these microglia. Also, my current investigation included only two of the originally planned five candidate miRNAs. Therefore, future studies aimed at studying the rest of the miRNAs and a combination of two-or-more miRNAs is needed to fully understand the supposed therapeutic potential of these miRNAs. Besides, experiments focusing on the impact of miRNAs on virus-associated factors could prove to be useful to delineate the mechanistic basis of miRNA-mediated reduction of virus replication. Also, since sterile inflammation did not produce a robust immune response in these cells, future work can be done to investigate if overexpression of these miRNAs has had any impact on the levels of TLR, NLRP and other proteins associated with these immune responses. This would grant us insight into the possible reasons for this weak response in the transduced HMC3 microglia.

While my project focused heavily on investigating the therapeutic potency of these miRNAs, the safety and efficacy of these miRNAs remain to be studied. Since miRNAs have been known to affect the expression of hundreds of genes, 'off-target' effects which stem from the usage of these miRNAs in therapy is a huge cause of concern and thus needs rigorous testing. Though 2D cell cultures are economical and less laborious, they fail to capture certain key aspects of more sophisticated structures like tissues, organs and organ systems. My results regarding 3D brain organoids, though preliminary, present an exciting opportunity for research with more advanced models than cell culture. The introduction of miR-expressing microglia into these 3D organoids will help recapitulate the CNS niche during latent HIV-1 infection and thus would prove to be a more useful model than conventional cell culture. As always, animal studies using either humanized mice or large animal models are needed to assess the safety, efficacy, and pharmacology of these miRNA therapeutics from an organismal perspective.

9.1.1 Identification of additional gene targets for use in HAND therapy

As mentioned earlier, only a couple of miRNA targets were investigated, which naturally lead us to look for other gene targets which might be helpful in HAND research. As a result, we decided to look at Illumina RNA microarray data obtained from PBMCs of participants from the Multicenter AIDS Cohort Study (MACS). The sample cohort consisted of 35 HIV- and 33 HIV+ patients (including one long term non-progressors [LTNP]). Of the HIV+ patients, 16 patients were HAND negative and 15 patients were HAND positive with varying levels of neurocognitive deficits. The quality control and downstream analysis of this microarray data were performed in RStudio using `lumi` and `limma` packages. The analysis requires the use of the original, unprocessed reads exported from the Illumina GeneStudio Software and a sample information sheet containing the information regarding the status of different variable (i.e. HIV/HAND status, CD4/CD8 counts etc.). Following quality control assessments and read normalization (which reduce the signal variation), a Bayesian statistical model was employed to identify the most significant differences in mRNA levels at a genome-wide false-discovery rate (FDR) less than either 0.05 (for HIV+ & HIV- cohort) and 0.1 (for HAND+ & HAND- cohort). Subsequently, a heatmap and TopTable representing the most significant hits were generated which are shown below.

- **HIV+ vs HIV- participants:**

Table 7: Top table with most significant hits between HIV+ and HIV- samples

Gene	*log(FC)*	*Fold change* ($2^{log(FC)}$)	*p<0.05 (Y/N)*
Homo sapiens apolipoprotein B mRNA editing enzyme, catalytic polypeptide-like 3G (APOBEC3G)	0.10585834	1.076134453	Y
Homo sapiens stomatin (STOM)	0.06810072	1.048335661	Y
Homo sapiens proteasome (prosome, macropain) subunit, alpha type, 6 (PSMA6)	0.09260457	1.066293479	Y
Homo sapiens zinc finger protein 66 (ZNF66)	-0.08153896	0.945049001	Y
Homo sapiens CD8a molecule (CD8A)	0.15990158	1.11721092	Y

Following the analysis, it is evident from the heatmap below that there is no discernable difference between HIV+ and HIV- participant samples. Also, the fold change of the 'statistically significant' hits is very low, and therefore making reliable conclusions regarding their 'practical significance' questionable. However, it is interesting to note that, a subset of HIV+ and HIV- people have a difference in the expression of CD8a protein. CD8a encodes the alpha chains of CD8 protein found on cytotoxic T-lymphocytes (CTLs) which helps mediate efficient interaction with antigen-MHC1 complex (217). This would mean that a subset of these individuals could have a more pronounced immune response to the virus than the rest of their cohort. Further analyses using additional patient samples and sensitive techniques like RNASeq could shed deeper insight into this phenomenon.

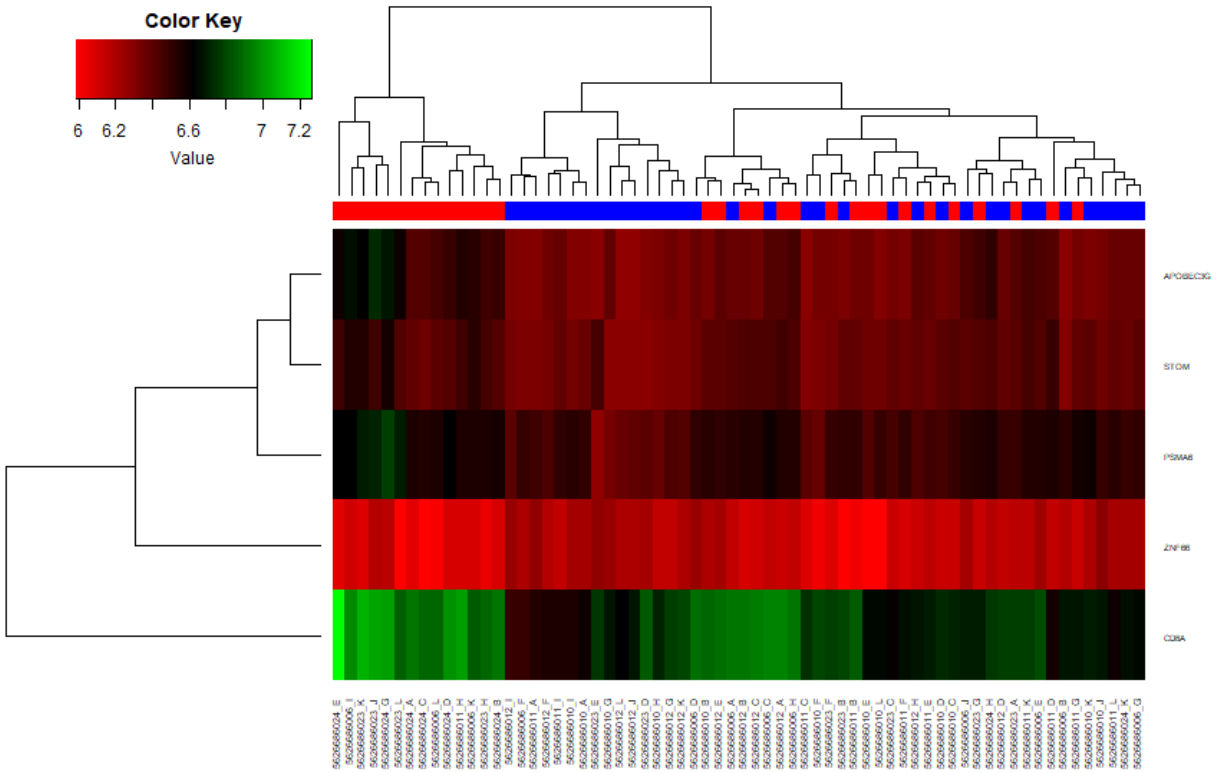

Figure 18: Heat-map showing differentially expressed genes in HIV+/HIV- samples: HIV+ and HIV- participants are represented by red and blue, respectively. All the hits represented here are FDR-adjusted to a significance level of less than 0.05.

- **HAND+ vs HAND- participants:**

Table 8: Top table with most significant hits between HAND+ and HAND- samples

Gene	*F value*	*p<0.1 (Y/N)*
Homo sapiens NPC1 (Niemann-Pick disease, type C1, gene)-like 1 (NPC1L1)	16.42692	Y
Homo sapiens apolipoprotein B mRNA editing enzyme, catalytic polypeptide-like 3G (APOBEC3G)	12.98036	N
Homo sapiens RAB27A, member RAS oncogene family (RAB27A)	13.59012	N
Homo sapiens stomatin (STOM)	14.75373	N

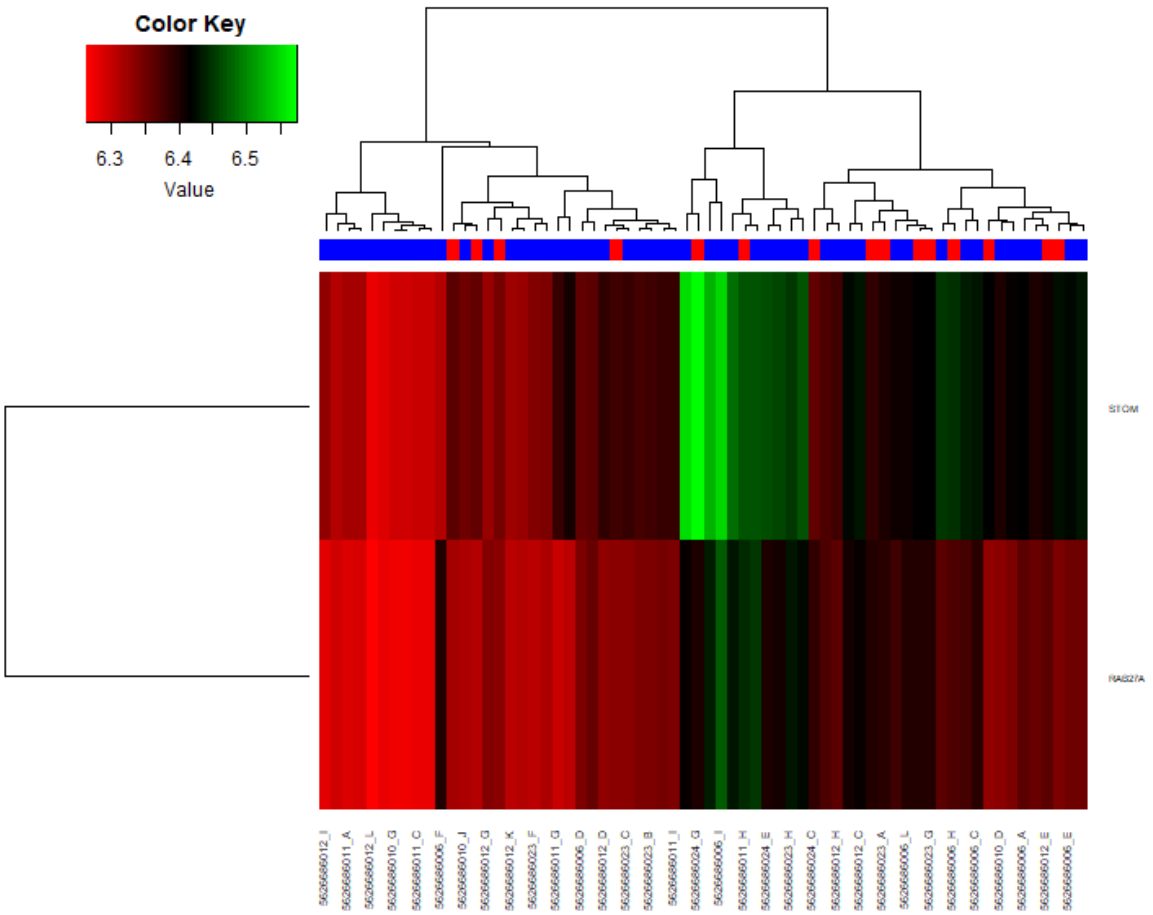

Figure 19: Heat-map showing differentially expressed genes in HAND+/HAND- samples: HAND+ and HAND- patients are represented by red and blue, respectively. All the hits represented here are FDR-adjusted to a significance level of less than 0.1.

Similar to the results from the HIV+ and HIV- cohort, microarray analysis between the subset of HAND+ and HAND- patients was incoherent. Additionally, only one gene candidate was found to be significantly different between the samples. This gene NPC1L1 encodes an enteric protein involved in cholesterol transport and absorption (218). The role of cholesterol and lipid rafts in aiding HIV-1 budding and release is widely known (219, 220); viral proteins like Nef have been reported to exploit this aspect for optimal infection (221). Thus, it is plausible that cholesterol transporters like NPC1L1 might affect virus replication, either positively or negatively. While

research into examining potential links between NPC1L1 and HIV-1 pathogenesis is scarce, there is evidence of role of NPC1L1 in other infectious diseases. For instance, Hepatitis C Virus (HCV) has been reported to use NPC1L1 as an accessory receptor for entry to cells (222). Ezetimibe, a lipid lowering medication, inhibits NPC1L1 activity (223, 224) and hence being investigated for use as an antiviral drug to combat HCV. Conclusively, research into targets like NPC1L1 might turn out to be important for better therapeutics to combat HIV-1 and HAND.

10.0 PUBLIC HEALTH SIGNIFICANCE

HIV-1 has been a major cause of public health concern since its inception in the 1980s. While it is true that combined antiretroviral therapy (cART)/highly active antiretroviral therapy (HAART) have been extremely effective at preventing the prognosis of acute HIV-1 infection to systemic, full-blown AIDS, the prevalence of other HIV-associated co-morbidities continues to be an issue among HIV+ patients. Of these co-morbidities, HIV-associated neurocognitive disorders (HAND) afflict nearly 50% of the infected cohort, albeit in a mild to moderate form in the post-cART era (8). These milder forms of HAND, which include asymptomatic neurocognitive impairment (ANI) and mild neurocognitive disorder (MND). As of now, there are no FDA-approved therapeutics to prevent, curb or even treat the pathogenesis of HAND. Furthermore, current antiviral therapies suffer from weak bioavailability beyond the blood-brain barrier (BBB), creating the exigent need for a newer class of antiretroviral therapeutics that can cross the BBB to prevent HIV-1 replication, if not HAND. Our work on these two miRNAs is a novel area of HIV-1 research which aim to reduce HIV-mediated inflammation and replication and consequently emerge as a new class of drugs to treat HAND. Consequently, our preliminary data indicate that both the miRNAs reduce inflammation during active HIV-1 infection. Also, miR-106b appears to hinder productive infection of HIV-1 as attested by flow cytometry and direct virus titers. Taken together, these preliminary results suggest that these miRNA candidates might have the potential to prevent neurodegeneration, cognitive dysfunction and other pathologies typically associated with HAND, thus deeming this avenue of research with extreme scope and significance in the field of public health.

BIBLIOGRAPHY

1. UNAIDS. 2019. Global HIV & AIDS statistics — 2019 fact sheet *on* UNAIDS. https://www.unaids.org/en/resources/fact-sheet.

2. Hankins C. 2013. Overview of the current state of the epidemic. Curr HIV/AIDS Rep 10:113-23.

3. Fettig J, Swaminathan M, Murrill CS, Kaplan JE. 2014. Global epidemiology of HIV. Infect Dis Clin North Am 28:323-37.

4. Williams BG, Lima V, Gouws E. 2011. Modelling the impact of antiretroviral therapy on the epidemic of HIV. Curr HIV Res 9:367-82.

5. Ahmed N. 2014. Most at-risk populations: contextualising HIV prevention programmes targeting marginalised groups in Zanzibar, Tanzania. Afr J AIDS Res 13:205-13.

6. Kellerman SE, Lehman JS, Lansky A, Stevens MR, Hecht FM, Bindman AB, Wortley PM. 2002. HIV testing within at-risk populations in the United States and the reasons for seeking or avoiding HIV testing. J Acquir Immune Defic Syndr 31:202-10.

7. Clifford DB, Ances BM. 2013. HIV-associated neurocognitive disorder. Lancet Infect Dis 13:976-86.

8. Heaton RK, Clifford DB, Franklin DR, Jr., Woods SP, Ake C, Vaida F, Ellis RJ, Letendre SL, Marcotte TD, Atkinson JH, Rivera-Mindt M, Vigil OR, Taylor MJ, Collier AC, Marra CM, Gelman BB, McArthur JC, Morgello S, Simpson DM, McCutchan JA, Abramson I, Gamst A, Fennema-Notestine C, Jernigan TL, Wong J, Grant I, Group C. 2010. HIV-associated neurocognitive disorders persist in the era of potent antiretroviral therapy: CHARTER Study. Neurology 75:2087-96.

9. Del Rio C. 2017. The global HIV epidemic: What the pathologist needs to know. Semin Diagn Pathol 34:314-317.

10. Simon V, Ho DD, Abdool Karim Q. 2006. HIV/AIDS epidemiology, pathogenesis, prevention, and treatment. Lancet 368:489-504.

11. Kilmarx PH. 2009. Global epidemiology of HIV. Curr Opin HIV AIDS 4:240-6.

12. WHO. 2018. HIV/AIDS: Data and Statistics. https://www.who.int/hiv/data/en/.

13. Blankenship KM, Smoyer AB, Bray SJ, Mattocks K. 2005. Black-white disparities in HIV/AIDS: the role of drug policy and the corrections system. J Health Care Poor Underserved 16:140-56.

14. Quinn TC, Wawer MJ, Sewankambo N, Serwadda D, Li C, Wabwire-Mangen F, Meehan MO, Lutalo T, Gray RH. 2000. Viral load and heterosexual transmission of human immunodeficiency virus type 1. Rakai Project Study Group. N Engl J Med 342:921-9.

15. Pilcher CD, Shugars DC, Fiscus SA, Miller WC, Menezes P, Giner J, Dean B, Robertson K, Hart CE, Lennox JL, Eron JJ, Jr., Hicks CB. 2001. HIV in body fluids during primary HIV infection: implications for pathogenesis, treatment and public health. AIDS 15:837-45.

16. Cohen MS, Gay CL. 2010. Treatment to prevent transmission of HIV-1. Clin Infect Dis 50 Suppl 3:S85-95.

17. Barre-Sinoussi F, Chermann JC, Rey F, Nugeyre MT, Chamaret S, Gruest J, Dauguet C, Axler-Blin C, Vezinet-Brun F, Rouzioux C, Rozenbaum W, Montagnier L. 1983. Isolation of a T-lymphotropic retrovirus from a patient at risk for acquired immune deficiency syndrome (AIDS). Science 220:868-71.

18. Popovic M, Sarngadharan MG, Read E, Gallo RC. 1984. Detection, isolation, and continuous production of cytopathic retroviruses (HTLV-III) from patients with AIDS and pre-AIDS. Science 224:497-500.

19. Luria SE. 1978. General Virology, 3rd ed. New York: Wiley.

20. Nyamweya S, Hegedus A, Jaye A, Rowland-Jones S, Flanagan KL, Macallan DC. 2013. Comparing HIV-1 and HIV-2 infection: Lessons for viral immunopathogenesis. Rev Med Virol 23:221-40.

21. Campbell-Yesufu OT, Gandhi RT. 2011. Update on human immunodeficiency virus (HIV)-2 infection. Clin Infect Dis 52:780-7.

22. Azevedo-Pereira JM, Santos-Costa Q. 2016. HIV Interaction With Human Host: HIV-2 As a Model of a Less Virulent Infection. AIDS Rev 18:44-53.

23. Frankel AD, Young JA. 1998. HIV-1: fifteen proteins and an RNA. Annu Rev Biochem 67:1-25.

24. Fanales-Belasio E, Raimondo M, Suligoi B, Butto S. 2010. HIV virology and pathogenetic mechanisms of infection: a brief overview. Ann Ist Super Sanita 46:5-14.

25. Briggs JA, Wilk T, Welker R, Krausslich HG, Fuller SD. 2003. Structural organization of authentic, mature HIV-1 virions and cores. EMBO J 22:1707-15.

26. Campbell EM, Hope TJ. 2015. HIV-1 capsid: the multifaceted key player in HIV-1 infection. Nat Rev Microbiol 13:471-83.

27. Göttlinger HG. HIV-1 Gag : a Molecular Machine Driving Viral Particle Assembly and Release.

28. Freed EO. 1998. HIV-1 gag proteins: diverse functions in the virus life cycle. Virology 251:1-15.

29. Picchio GR, Gulizia RJ, Wehrly K, Chesebro B, Mosier DE. 1998. The cell tropism of human immunodeficiency virus type 1 determines the kinetics of plasma viremia in SCID mice reconstituted with human peripheral blood leukocytes. J Virol 72:2002-9.

30. Poveda E, Briz V, Quinones-Mateu M, Soriano V. 2006. HIV tropism: diagnostic tools and implications for disease progression and treatment with entry inhibitors. AIDS 20:1359-67.

31. McKenna PM, Pomerantz RJ, Dietzschold B, McGettigan JP, Schnell MJ. 2003. Covalently linked human immunodeficiency virus type 1 gp120/gp41 is stably anchored in rhabdovirus particles and exposes critical neutralizing epitopes. J Virol 77:12782-94.

32. Rychert J, Strick D, Bazner S, Robinson J, Rosenberg E. 2010. Detection of HIV gp120 in plasma during early HIV infection is associated with increased proinflammatory and immunoregulatory cytokines. AIDS Res Hum Retroviruses 26:1139-45.

33. Rice AP. 2017. The HIV-1 Tat Protein: Mechanism of Action and Target for HIV-1 Cure Strategies. Curr Pharm Des 23:4098-4102.

34. Emiliani S, Fischle W, Ott M, Van Lint C, Amella CA, Verdin E. 1998. Mutations in the tat gene are responsible for human immunodeficiency virus type 1 postintegration latency in the U1 cell line. J Virol 72:1666-70.

35. Pollard VW, Malim MH. 1998. The HIV-1 Rev protein. Annu Rev Microbiol 52:491-532.

36. Fernandes J, Jayaraman B, Frankel A. 2012. The HIV-1 Rev response element: an RNA scaffold that directs the cooperative assembly of a homo-oligomeric ribonucleoprotein complex. RNA Biol 9:6-11.

37. Cochrane A, Kramer R, Ruben S, Levine J, Rosen CA. 1989. The human immunodeficiency virus rev protein is a nuclear phosphoprotein. Virology 171:264-6.

38. Jeong KS, Nam YS, Venkatesan S. 2000. Deletions near the N-terminus of HIV-1 Rev reduce RNA binding affinity and dominantly interfere with Rev function irrespective of the RNA target. Arch Virol 145:2443-67.

39. Daly TJ, Rennert P, Lynch P, Barry JK, Dundas M, Rusche JR, Doten RC, Auer M, Farrington GK. 1993. Perturbation of the carboxy terminus of HIV-1 Rev affects multimerization on the Rev responsive element. Biochemistry 32:8945-54.

40. Daly TJ, Doten RC, Rusche JR, Auer M. 1995. The amino terminal domain of HIV-1 Rev is required for discrimination of the RRE from nonspecific RNA. J Mol Biol 253:243-58.

41. Greatorex JS, Palmer EA, Pomerantz RJ, Dangerfield JA, Lever AM. 2006. Mutation of the Rev-binding loop in the human immunodeficiency virus 1 leader causes a replication defect characterized by altered RNA trafficking and packaging. J Gen Virol 87:3039-44.

42. Ragheb JA, Bressler P, Daucher M, Chiang L, Chuah MK, VandenDriessche T, Morgan RA. 1995. Analysis of trans-dominant mutants of the HIV type 1 Rev protein for their ability to inhibit Rev function, HIV type 1 replication, and their use as anti-HIV gene therapeutics. AIDS Res Hum Retroviruses 11:1343-53.

43. Malim MH, Emerman M. 2008. HIV-1 accessory proteins--ensuring viral survival in a hostile environment. Cell Host Microbe 3:388-98.

44. Papa F, Binda F, Felici G, Franzetti M, Gandolfi A, Sinisgalli C, Balotta C. 2018. A simple model of HIV epidemic in Italy: The role of the antiretroviral treatment. Math Biosci Eng 15:181-207.

45. Yan N, Chen ZJ. 2012. Intrinsic antiviral immunity. Nat Immunol 13:214-22.

46. Messaoudi I, Amarasinghe GK, Basler CF. 2015. Filovirus pathogenesis and immune evasion: insights from Ebola virus and Marburg virus. Nat Rev Microbiol 13:663-76.

47. van de Sandt CE, Kreijtz JH, Rimmelzwaan GF. 2012. Evasion of influenza A viruses from innate and adaptive immune responses. Viruses 4:1438-76.

48. Goon PK, Bangham CR. 2004. Interference with immune function by HTLV-1. Clin Exp Immunol 137:234-6.

49. Guha D, Ayyavoo V. 2013. Innate immune evasion strategies by human immunodeficiency virus type 1. ISRN AIDS 2013:954806.

50. Cosnefroy O, Murray PJ, Bishop KN. 2016. HIV-1 capsid uncoating initiates after the first strand transfer of reverse transcription. Retrovirology 13:58.

51. Das SR, Jameel S. 2005. Biology of the HIV Nef protein. Indian J Med Res 121:315-32.

52. Dube M, Bego MG, Paquay C, Cohen EA. 2010. Modulation of HIV-1-host interaction: role of the Vpu accessory protein. Retrovirology 7:114.

53. Gonzalez ME. 2017. The HIV-1 Vpr Protein: A Multifaceted Target for Therapeutic Intervention. Int J Mol Sci 18.

54. Wilen CB, Tilton JC, Doms RW. 2012. HIV: cell binding and entry. Cold Spring Harb Perspect Med 2.

55. Kowalska JD, Wojcik G, Rutkowski J, Ankiersztejn-Bartczak M, Siewaszewicz E. 2017. Modelling the cost-effectiveness of HIV care shows a clear benefit when transmission risk is considered in the calculations - A message for Central and Eastern Europe. PLoS One 12:e0186131.

56. Ambrose Z, Aiken C. 2014. HIV-1 uncoating: connection to nuclear entry and regulation by host proteins. Virology 454-455:371-9.

57. Hulme AE, Kelley Z, Okocha EA, Hope TJ. 2015. Identification of capsid mutations that alter the rate of HIV-1 uncoating in infected cells. J Virol 89:643-51.

58. Hulme AE, Perez O, Hope TJ. 2011. Complementary assays reveal a relationship between HIV-1 uncoating and reverse transcription. Proc Natl Acad Sci U S A 108:9975-80.

59. Rankovic S, Varadarajan J, Ramalho R, Aiken C, Rousso I. 2017. Reverse Transcription Mechanically Initiates HIV-1 Capsid Disassembly. J Virol 91.

60. Baltimore D. 1970. RNA-dependent DNA polymerase in virions of RNA tumour viruses. Nature 226:1209-11.

61. Mizutani S, Boettiger D, Temin HM. 1970. A DNA-depenent DNA polymerase and a DNA endonuclease in virions of Rous sarcoma virus. Nature 228:424-7.

62. Tian L, Kim MS, Li H, Wang J, Yang W. 2018. Structure of HIV-1 reverse transcriptase cleaving RNA in an RNA/DNA hybrid. Proc Natl Acad Sci U S A 115:507-512.

63. Sarafianos SG, Marchand B, Das K, Himmel DM, Parniak MA, Hughes SH, Arnold E. 2009. Structure and function of HIV-1 reverse transcriptase: molecular mechanisms of polymerization and inhibition. J Mol Biol 385:693-713.

64. Hu WS, Hughes SH. 2012. HIV-1 reverse transcription. Cold Spring Harb Perspect Med 2.

65. Arhel N. 2010. Revisiting HIV-1 uncoating. Retrovirology 7:96.

66. Blankson JN, Siliciano JD, Siliciano RF. 2014. Finding a cure for human immunodeficiency virus-1 infection. Infect Dis Clin North Am 28:633-50.

67. Hill M, Tachedjian G, Mak J. 2005. The packaging and maturation of the HIV-1 Pol proteins. Curr HIV Res 3:73-85.

68. Chiu TK, Davies DR. 2004. Structure and function of HIV-1 integrase. Curr Top Med Chem 4:965-77.

69. Craigie R, Bushman FD. 2012. HIV DNA integration. Cold Spring Harb Perspect Med 2:a006890.

70. Engelman AN, Singh PK. 2018. Cellular and molecular mechanisms of HIV-1 integration targeting. Cell Mol Life Sci 75:2491-2507.

71. Schroder AR, Shinn P, Chen H, Berry C, Ecker JR, Bushman F. 2002. HIV-1 integration in the human genome favors active genes and local hotspots. Cell 110:521-9.

72. Mitchell RS, Beitzel BF, Schroder AR, Shinn P, Chen H, Berry CC, Ecker JR, Bushman FD. 2004. Retroviral DNA integration: ASLV, HIV, and MLV show distinct target site preferences. PLoS Biol 2:E234.

73. Lusic M, Siliciano RF. 2017. Nuclear landscape of HIV-1 infection and integration. Nat Rev Microbiol 15:69-82.

74. Sundquist WI, Krausslich HG. 2012. HIV-1 assembly, budding, and maturation. Cold Spring Harb Perspect Med 2:a006924.

75. Göttlinger H. 2013. Advances in HIV-1 Assembly and Release doi:https://doi.org/10.1007/978-1-4614-7729-7_5. Springer, New York, NY.

76. Weiss ER, Gottlinger H. 2011. The role of cellular factors in promoting HIV budding. J Mol Biol 410:525-33.

77. Brik A, Wong CH. 2003. HIV-1 protease: mechanism and drug discovery. Org Biomol Chem 1:5-14.

78. Ghosh AK, Osswald HL, Prato G. 2016. Recent Progress in the Development of HIV-1 Protease Inhibitors for the Treatment of HIV/AIDS. J Med Chem 59:5172-208.

79. Freed EO. 2015. HIV-1 assembly, release and maturation. Nat Rev Microbiol 13:484-96.

80. Daneman R, Prat A. 2015. The blood-brain barrier. Cold Spring Harb Perspect Biol 7:a020412.

81. Ene L. 2018. Human Immunodeficiency Virus in the Brain-Culprit or Facilitator? Infect Dis (Auckl) 11:1178633717752687.

82. Spudich S, Gonzalez-Scarano F. 2012. HIV-1-related central nervous system disease: current issues in pathogenesis, diagnosis, and treatment. Cold Spring Harb Perspect Med 2:a007120.

83. Gisolf EH, van Praag RM, Jurriaans S, Portegies P, Goudsmit J, Danner SA, Lange JM, Prins JM. 2000. Increasing cerebrospinal fluid chemokine concentrations despite undetectable cerebrospinal fluid HIV RNA in HIV-1-infected patients receiving antiretroviral therapy. J Acquir Immune Defic Syndr 25:426-33.

84. Canestri A, Lescure FX, Jaureguiberry S, Moulignier A, Amiel C, Marcelin AG, Peytavin G, Tubiana R, Pialoux G, Katlama C. 2010. Discordance between cerebral spinal fluid and plasma HIV replication in patients with neurological symptoms who are receiving suppressive antiretroviral therapy. Clin Infect Dis 50:773-8.

85. Dravid AN, Natrajan K, Kulkarni MM, Saraf CK, Mahajan US, Kore SD, Rathod NM, Mahajan US, Wadia RS. 2018. Discordant CSF/plasma HIV-1 RNA in individuals on virologically suppressive antiretroviral therapy in Western India. Medicine (Baltimore) 97:e9969.

86. Nightingale S, Geretti AM, Beloukas A, Fisher M, Winston A, Else L, Nelson M, Taylor S, Ustianowski A, Ainsworth J, Gilson R, Haddow L, Ong E, Watson V, Leen C, Minton

J, Post F, Pirmohamed M, Solomon T, Khoo S. 2016. Discordant CSF/plasma HIV-1 RNA in patients with unexplained low-level viraemia. J Neurovirol 22:852-860.

87. Reu P, Khosravi A, Bernard S, Mold JE, Salehpour M, Alkass K, Perl S, Tisdale J, Possnert G, Druid H, Frisen J. 2017. The Lifespan and Turnover of Microglia in the Human Brain. Cell Rep 20:779-784.

88. Antinori A, Arendt G, Becker JT, Brew BJ, Byrd DA, Cherner M, Clifford DB, Cinque P, Epstein LG, Goodkin K, Gisslen M, Grant I, Heaton RK, Joseph J, Marder K, Marra CM, McArthur JC, Nunn M, Price RW, Pulliam L, Robertson KR, Sacktor N, Valcour V, Wojna VE. 2007. Updated research nosology for HIV-associated neurocognitive disorders. Neurology 69:1789-99.

89. Saylor D, Dickens AM, Sacktor N, Haughey N, Slusher B, Pletnikov M, Mankowski JL, Brown A, Volsky DJ, McArthur JC. 2016. HIV-associated neurocognitive disorder--pathogenesis and prospects for treatment. Nat Rev Neurol 12:234-48.

90. McArthur JC, Steiner J, Sacktor N, Nath A. 2010. Human immunodeficiency virus-associated neurocognitive disorders: Mind the gap. Ann Neurol 67:699-714.

91. Rao VR, Ruiz AP, Prasad VR. 2014. Viral and cellular factors underlying neuropathogenesis in HIV associated neurocognitive disorders (HAND). AIDS Res Ther 11:13.

92. Ballester LY, Capo-Velez CM, Garcia-Beltran WF, Ramos FM, Vazquez-Rosa E, Rios R, Mercado JR, Melendez RI, Lasalde-Dominicci JA. 2012. Up-regulation of the neuronal nicotinic receptor alpha7 by HIV glycoprotein 120: potential implications for HIV-associated neurocognitive disorder. J Biol Chem 287:3079-86.

93. Kaul M, Lipton SA. 1999. Chemokines and activated macrophages in HIV gp120-induced neuronal apoptosis. Proc Natl Acad Sci U S A 96:8212-6.

94. Lannuzel A, Lledo PM, Lamghitnia HO, Vincent JD, Tardieu M. 1995. HIV-1 envelope proteins gp120 and gp160 potentiate NMDA-induced [Ca2+]i increase, alter [Ca2+]i homeostasis and induce neurotoxicity in human embryonic neurons. Eur J Neurosci 7:2285-93.

95. Haughey NJ, Holden CP, Nath A, Geiger JD. 1999. Involvement of inositol 1,4,5-trisphosphate-regulated stores of intracellular calcium in calcium dysregulation and neuron cell death caused by HIV-1 protein tat. J Neurochem 73:1363-74.

96. Nath A, Psooy K, Martin C, Knudsen B, Magnuson DS, Haughey N, Geiger JD. 1996. Identification of a human immunodeficiency virus type 1 Tat epitope that is neuroexcitatory and neurotoxic. J Virol 70:1475-80.

97. Zhu J, Ananthan S, Mactutus CF, Booze RM. 2011. Recombinant human immunodeficiency virus-1 transactivator of transcription1-86 allosterically modulates dopamine transporter activity. Synapse 65:1251-4.

98. Williams DW, Veenstra M, Gaskill PJ, Morgello S, Calderon TM, Berman JW. 2014. Monocytes mediate HIV neuropathogenesis: mechanisms that contribute to HIV associated neurocognitive disorders. Curr HIV Res 12:85-96.

99. Bachiller S, Jimenez-Ferrer I, Paulus A, Yang Y, Swanberg M, Deierborg T, Boza-Serrano A. 2018. Microglia in Neurological Diseases: A Road Map to Brain-Disease Dependent-Inflammatory Response. Front Cell Neurosci 12:488.

100. Ginhoux F, Prinz M. 2015. Origin of microglia: current concepts and past controversies. Cold Spring Harb Perspect Biol 7:a020537.

101. Burdo TH, Lackner A, Williams KC. 2013. Monocyte/macrophages and their role in HIV neuropathogenesis. Immunol Rev 254:102-13.

102. Takeuchi O, Akira S. 2010. Pattern recognition receptors and inflammation. Cell 140:805-20.

103. Zhang L, Zhang J, You Z. 2018. Switching of the Microglial Activation Phenotype Is a Possible Treatment for Depression Disorder. Front Cell Neurosci 12:306.

104. Zhao ML, Kim MO, Morgello S, Lee SC. 2001. Expression of inducible nitric oxide synthase, interleukin-1 and caspase-1 in HIV-1 encephalitis. J Neuroimmunol 115:182-91.

105. Clouse KA, Cosentino LM, Weih KA, Pyle SW, Robbins PB, Hochstein HD, Natarajan V, Farrar WL. 1991. The HIV-1 gp120 envelope protein has the intrinsic capacity to stimulate monokine secretion. J Immunol 147:2892-901.

106. Walsh JG, Reinke SN, Mamik MK, McKenzie BA, Maingat F, Branton WG, Broadhurst DI, Power C. 2014. Rapid inflammasome activation in microglia contributes to brain disease in HIV/AIDS. Retrovirology 11:35.

107. Kany S, Vollrath JT, Relja B. 2019. Cytokines in Inflammatory Disease. Int J Mol Sci 20.

108. Nicolini A, Ajmone-Cat MA, Bernardo A, Levi G, Minghetti L. 2001. Human immunodeficiency virus type-1 Tat protein induces nuclear factor (NF)-kappaB activation and oxidative stress in microglial cultures by independent mechanisms. J Neurochem 79:713-6.

109. Nookala AR, Kumar A. 2014. Molecular mechanisms involved in HIV-1 Tat-mediated induction of IL-6 and IL-8 in astrocytes. J Neuroinflammation 11:214.

110. Sharief MK, Ciardi M, Noori MA, Thompson EJ, Salotti A, Sorice F, Rossi F, Cirelli A. 1992. Free circulating ICAM-1 in serum and cerebrospinal fluid of HIV-1 infected patients correlate with TNF-alpha and blood-brain barrier damage. Mediators Inflamm 1:323-8.

111. Tong N, Perry SW, Zhang Q, James HJ, Guo H, Brooks A, Bal H, Kinnear SA, Fine S, Epstein LG, Dairaghi D, Schall TJ, Gendelman HE, Dewhurst S, Sharer LR, Gelbard HA.

2000. Neuronal fractalkine expression in HIV-1 encephalitis: roles for macrophage recruitment and neuroprotection in the central nervous system. J Immunol 164:1333-9.

112. Williams KC, Corey S, Westmoreland SV, Pauley D, Knight H, deBakker C, Alvarez X, Lackner AA. 2001. Perivascular macrophages are the primary cell type productively infected by simian immunodeficiency virus in the brains of macaques: implications for the neuropathogenesis of AIDS. J Exp Med 193:905-15.

113. Bezzi P, Domercq M, Brambilla L, Galli R, Schols D, De Clercq E, Vescovi A, Bagetta G, Kollias G, Meldolesi J, Volterra A. 2001. CXCR4-activated astrocyte glutamate release via TNFalpha: amplification by microglia triggers neurotoxicity. Nat Neurosci 4:702-10.

114. Jiang ZG, Piggee C, Heyes MP, Murphy C, Quearry B, Bauer M, Zheng J, Gendelman HE, Markey SP. 2001. Glutamate is a mediator of neurotoxicity in secretions of activated HIV-1-infected macrophages. J Neuroimmunol 117:97-107.

115. Atlas A, Gisslen M, Nordin C, Lindstrom L, Schwieler L. 2007. Acute psychotic symptoms in HIV-1 infected patients are associated with increased levels of kynurenic acid in cerebrospinal fluid. Brain Behav Immun 21:86-91.

116. Erdmann N, Zhao J, Lopez AL, Herek S, Curthoys N, Hexum TD, Tsukamoto T, Ferraris D, Zheng J. 2007. Glutamate production by HIV-1 infected human macrophage is blocked by the inhibition of glutaminase. J Neurochem 102:539-49.

117. Ferrarese C, Aliprandi A, Tremolizzo L, Stanzani L, De Micheli A, Dolara A, Frattola L. 2001. Increased glutamate in CSF and plasma of patients with HIV dementia. Neurology 57:671-5.

118. Breen EC, Rezai AR, Nakajima K, Beall GN, Mitsuyasu RT, Hirano T, Kishimoto T, Martinez-Maza O. 1990. Infection with HIV is associated with elevated IL-6 levels and production. J Immunol 144:480-4.

119. Borges AH, O'Connor JL, Phillips AN, Ronsholt FF, Pett S, Vjecha MJ, French MA, Lundgren JD, Insight S, Groups ES, the SSC. 2015. Factors Associated With Plasma IL-6 Levels During HIV Infection. J Infect Dis 212:585-95.

120. Yuan L, Qiao L, Wei F, Yin J, Liu L, Ji Y, Smith D, Li N, Chen D. 2013. Cytokines in CSF correlate with HIV-associated neurocognitive disorders in the post-HAART era in China. J Neurovirol 19:144-9.

121. Matsumoto T, Miike T, Nelson RP, Trudeau WL, Lockey RF, Yodoi J. 1993. Elevated serum levels of IL-8 in patients with HIV infection. Clin Exp Immunol 93:149-51.

122. Lander ES, Linton LM, Birren B, Nusbaum C, Zody MC, Baldwin J, Devon K, Dewar K, Doyle M, FitzHugh W, Funke R, Gage D, Harris K, Heaford A, Howland J, Kann L, Lehoczky J, LeVine R, McEwan P, McKernan K, Meldrim J, Mesirov JP, Miranda C, Morris W, Naylor J, Raymond C, Rosetti M, Santos R, Sheridan A, Sougnez C, Stange-Thomann Y, Stojanovic N, Subramanian A, Wyman D, Rogers J, Sulston J, Ainscough R,

Beck S, Bentley D, Burton J, Clee C, Carter N, Coulson A, Deadman R, Deloukas P, Dunham A, Dunham I, Durbin R, French L, Grafham D, et al. 2001. Initial sequencing and analysis of the human genome. Nature 409:860-921.

123. International Human Genome Sequencing C. 2004. Finishing the euchromatic sequence of the human genome. Nature 431:931-45.

124. Patrushev LI, Kovalenko TF. 2014. Functions of noncoding sequences in mammalian genomes. Biochemistry (Mosc) 79:1442-69.

125. Palazzo AF, Lee ES. 2015. Non-coding RNA: what is functional and what is junk? Front Genet 6:2.

126. Watson CN, Belli A, Di Pietro V. 2019. Small Non-coding RNAs: New Class of Biomarkers and Potential Therapeutic Targets in Neurodegenerative Disease. Front Genet 10:364.

127. Jaenisch R, Bird A. 2003. Epigenetic regulation of gene expression: how the genome integrates intrinsic and environmental signals. Nat Genet 33 Suppl:245-54.

128. Gibney ER, Nolan CM. 2010. Epigenetics and gene expression. Heredity (Edinb) 105:4-13.

129. Lee TI, Young RA. 2013. Transcriptional regulation and its misregulation in disease. Cell 152:1237-51.

130. Carthew RW, Sontheimer EJ. 2009. Origins and Mechanisms of miRNAs and siRNAs. Cell 136:642-55.

131. Han J, Lee Y, Yeom KH, Kim YK, Jin H, Kim VN. 2004. The Drosha-DGCR8 complex in primary microRNA processing. Genes Dev 18:3016-27.

132. Okada C, Yamashita E, Lee SJ, Shibata S, Katahira J, Nakagawa A, Yoneda Y, Tsukihara T. 2009. A high-resolution structure of the pre-microRNA nuclear export machinery. Science 326:1275-9.

133. Denli AM, Tops BB, Plasterk RH, Ketting RF, Hannon GJ. 2004. Processing of primary microRNAs by the Microprocessor complex. Nature 432:231-5.

134. Yoda M, Kawamata T, Paroo Z, Ye X, Iwasaki S, Liu Q, Tomari Y. 2010. ATP-dependent human RISC assembly pathways. Nat Struct Mol Biol 17:17-23.

135. O'Brien J, Hayder H, Zayed Y, Peng C. 2018. Overview of MicroRNA Biogenesis, Mechanisms of Actions, and Circulation. Front Endocrinol (Lausanne) 9:402.

136. Guessous F, Alvarado-Velez M, Marcinkiewicz L, Zhang Y, Kim J, Heister S, Kefas B, Godlewski J, Schiff D, Purow B, Abounader R. 2013. Oncogenic effects of miR-10b in glioblastoma stem cells. J Neurooncol 112:153-63.

137. Zhen L, Li J, Zhang M, Yang K. 2016. MiR-10b decreases sensitivity of glioblastoma cells to radiation by targeting AKT. J Biol Res (Thessalon) 23:14.

138. Buruiana A, Florian SI, Florian AI, Timis TL, Mihu CM, Miclaus M, Osan S, Hrapsa I, Cataniciu RC, Farcas M, Susman S. 2020. The Roles of miRNA in Glioblastoma Tumor Cell Communication: Diplomatic and Aggressive Negotiations. Int J Mol Sci 21.

139. Jiang K, Hu J, Luo G, Song D, Zhang P, Zhu J, Sun F. 2020. miR-155-5p Promotes Oxalate- and Calcium-Induced Kidney Oxidative Stress Injury by Suppressing MGP Expression. Oxid Med Cell Longev 2020:5863617.

140. Lan C, Chen D, Liang X, Huang J, Zeng T, Duan X, Chen K, Lai Y, Yang D, Li S, Jiang C, Wu W. 2017. Integrative Analysis of miRNA and mRNA Expression Profiles in Calcium Oxalate Nephrolithiasis Rat Model. Biomed Res Int 2017:8306736.

141. Schult P, Roth H, Adams RL, Mas C, Imbert L, Orlik C, Ruggieri A, Pyle AM, Lohmann V. 2018. microRNA-122 amplifies hepatitis C virus translation by shaping the structure of the internal ribosomal entry site. Nat Commun 9:2613.

142. Jopling CL, Yi M, Lancaster AM, Lemon SM, Sarnow P. 2005. Modulation of hepatitis C virus RNA abundance by a liver-specific MicroRNA. Science 309:1577-81.

143. Ding L, Xu Y, Zhang W, Deng Y, Si M, Du Y, Yao H, Liu X, Ke Y, Si J, Zhou T. 2010. MiR-375 frequently downregulated in gastric cancer inhibits cell proliferation by targeting JAK2. Cell Res 20:784-93.

144. Huang ZS, Guo XW, Zhang G, Liang LX, Nong B. 2019. The Diagnostic and Prognostic Value of miR-200c in Gastric Cancer: A Meta-Analysis. Dis Markers 2019:8949618.

145. Fomison-Nurse I, Saw EEL, Gandhi S, Munasinghe PE, Van Hout I, Williams MJA, Galvin I, Bunton R, Davis P, Cameron V, Katare R. 2018. Diabetes induces the activation of pro-ageing miR-34a in the heart, but has differential effects on cardiomyocytes and cardiac progenitor cells. Cell Death Differ 25:1336-1349.

146. Desjarlais M, Wirth M, Rivera JC, Lahaie I, Dabouz R, Omri S, Ruknudin P, Borras C, Chemtob S. 2020. MicroRNA-96 Promotes Vascular Repair in Oxygen-Induced Retinopathy-A Novel Uncovered Vasoprotective Function. Front Pharmacol 11:13.

147. Martinez B, Peplow PV. 2019. MicroRNAs as biomarkers of diabetic retinopathy and disease progression. Neural Regen Res 14:1858-1869.

148. Rayner KJ, Sheedy FJ, Esau CC, Hussain FN, Temel RE, Parathath S, van Gils JM, Rayner AJ, Chang AN, Suarez Y, Fernandez-Hernando C, Fisher EA, Moore KJ. 2011. Antagonism of miR-33 in mice promotes reverse cholesterol transport and regression of atherosclerosis. J Clin Invest 121:2921-31.

149. Liu K, Xuekelati S, Zhang Y, Yin Y, Li Y, Chai R, Li X, Peng Y, Wu J, Guo X. 2017. Expression levels of atherosclerosis-associated miR-143 and miR-145 in the plasma of patients with hyperhomocysteinaemia. BMC Cardiovasc Disord 17:163.

150. Lin X, Rice KL, Buzzai M, Hexner E, Costa FF, Kilpivaara O, Mullally A, Soares MB, Ebert BL, Levine R, Licht JD. 2013. miR-433 is aberrantly expressed in myeloproliferative neoplasms and suppresses hematopoietic cell growth and differentiation. Leukemia 27:344-52.

151. Tombak A, Ay OI, Erdal ME, Sungur MA, Ucar MA, Akdeniz A, Tiftik EN. 2015. MicroRNA Expression Analysis in Patients with Primary Myelofibrosis, Polycythemia vera and Essential Thrombocythemia. Indian J Hematol Blood Transfus 31:416-25.

152. Takaki Y, Saito Y, Takasugi A, Toshimitsu K, Yamada S, Muramatsu T, Kimura M, Sugiyama K, Suzuki H, Arai E, Ojima H, Kanai Y, Saito H. 2014. Silencing of microRNA-122 is an early event during hepatocarcinogenesis from non-alcoholic steatohepatitis. Cancer Sci 105:1254-60.

153. Xu J, Wu C, Che X, Wang L, Yu D, Zhang T, Huang L, Li H, Tan W, Wang C, Lin D. 2011. Circulating microRNAs, miR-21, miR-122, and miR-223, in patients with hepatocellular carcinoma or chronic hepatitis. Mol Carcinog 50:136-42.

154. Baumann V, Winkler J. 2014. miRNA-based therapies: strategies and delivery platforms for oligonucleotide and non-oligonucleotide agents. Future Med Chem 6:1967-84.

155. Lennox KA, Behlke MA. 2011. Chemical modification and design of anti-miRNA oligonucleotides. Gene Ther 18:1111-20.

156. Bramsen JB, Laursen MB, Nielsen AF, Hansen TB, Bus C, Langkjaer N, Babu BR, Hojland T, Abramov M, Van Aerschot A, Odadzic D, Smicius R, Haas J, Andree C, Barman J, Wenska M, Srivastava P, Zhou C, Honcharenko D, Hess S, Muller E, Bobkov GV, Mikhailov SN, Fava E, Meyer TF, Chattopadhyaya J, Zerial M, Engels JW, Herdewijn P, Wengel J, Kjems J. 2009. A large-scale chemical modification screen identifies design rules to generate siRNAs with high activity, high stability and low toxicity. Nucleic Acids Res 37:2867-81.

157. Zhang Y, Wang Z, Gemeinhart RA. 2013. Progress in microRNA delivery. J Control Release 172:962-74.

158. Adams D, Gonzalez-Duarte A, O'Riordan WD, Yang CC, Ueda M, Kristen AV, Tournev I, Schmidt HH, Coelho T, Berk JL, Lin KP, Vita G, Attarian S, Plante-Bordeneuve V, Mezei MM, Campistol JM, Buades J, Brannagan TH, 3rd, Kim BJ, Oh J, Parman Y, Sekijima Y, Hawkins PN, Solomon SD, Polydefkis M, Dyck PJ, Gandhi PJ, Goyal S, Chen J, Strahs AL, Nochur SV, Sweetser MT, Garg PP, Vaishnaw AK, Gollob JA, Suhr OB. 2018. Patisiran, an RNAi Therapeutic, for Hereditary Transthyretin Amyloidosis. N Engl J Med 379:11-21.

159. Rupaimoole R, Slack FJ. 2017. MicroRNA therapeutics: towards a new era for the management of cancer and other diseases. Nat Rev Drug Discov 16:203-222.

160. Venkatachari NJ, Jain S, Walker L, Bivalkar-Mehla S, Chattopadhyay A, Bar-Joseph Z, Rinaldo C, Ragin A, Seaberg E, Levine A, Becker J, Martin E, Sacktor N, Ayyavoo V. 2017. Transcriptome analyses identify key cellular factors associated with HIV-1-associated neuropathogenesis in infected men. AIDS 31:623-633.

161. Cairomicron O. 2011. External measures of cognition. Front Hum Neurosci 5:108.

162. Harrison RG. 1906. Observations on the living developing nerve fiber. Proceedings of the Society for Experimental Biology and Medicine 4:140-143.

163. Millet LJ, Gillette MU. 2012. Over a century of neuron culture: from the hanging drop to microfluidic devices. Yale J Biol Med 85:501-21.

164. Aref'eva AM, Gutkina AV, Enenko SO, Shungskaya VE. 1966. In vivo investigation of nerve cells surviving in tissue culture by method of fluorescence analysis. Fed Proc Transl Suppl 25:953-6.

165. Kim SU. 1966. Histochemical demonstration of oxidative enzymes associated with carbohydrate metabolism in cerebellar neurons cultured in vitro. Arch Histol Jpn 27:465-71.

166. Johnson L, Morrow J, Kasten FH, DiZerega G. 1970. Isolation of viable neurons from embryonic spinal ganglia by centrifugation through albumin gradients. Exp Cell Res 63:189-92.

167. Chen JS, Levi-Montalcini R. 1970. Long term cultures of dissociated nerve cells from the embryonic nervous system of the cockroach Periplaneta americana. Arch Ital Biol 108:503-37.

168. Gordon J, Amini S, White MK. 2013. General overview of neuronal cell culture. Methods Mol Biol 1078:1-8.

169. Thomson JA, Itskovitz-Eldor J, Shapiro SS, Waknitz MA, Swiergiel JJ, Marshall VS, Jones JM. 1998. Embryonic stem cell lines derived from human blastocysts. Science 282:1145-7.

170. Takahashi K, Tanabe K, Ohnuki M, Narita M, Ichisaka T, Tomoda K, Yamanaka S. 2007. Induction of pluripotent stem cells from adult human fibroblasts by defined factors. Cell 131:861-72.

171. Yu J, Vodyanik MA, Smuga-Otto K, Antosiewicz-Bourget J, Frane JL, Tian S, Nie J, Jonsdottir GA, Ruotti V, Stewart R, Slukvin, II, Thomson JA. 2007. Induced pluripotent stem cell lines derived from human somatic cells. Science 318:1917-20.

172. Johnson BV, Shindo N, Rathjen PD, Rathjen J, Keough RA. 2008. Understanding pluripotency—how embryonic stem cells keep their options open. Molecular Human Reproduction 14:513-520.

173. Zhang SC, Wernig M, Duncan ID, Brustle O, Thomson JA. 2001. In vitro differentiation of transplantable neural precursors from human embryonic stem cells. Nat Biotechnol 19:1129-33.

174. Shi Y, Kirwan P, Smith J, Robinson HP, Livesey FJ. 2012. Human cerebral cortex development from pluripotent stem cells to functional excitatory synapses. Nat Neurosci 15:477-86, S1.

175. Murry CE, Keller G. 2008. Differentiation of embryonic stem cells to clinically relevant populations: lessons from embryonic development. Cell 132:661-80.

176. Medvedev SP, Shevchenko AI, Zakian SM. 2010. Induced Pluripotent Stem Cells: Problems and Advantages when Applying them in Regenerative Medicine. Acta Naturae 2:18-28.

177. Pacitti D, Privolizzi R, Bax BE. 2019. Organs to Cells and Cells to Organoids: The Evolution of in vitro Central Nervous System Modelling. Front Cell Neurosci 13:129.

178. Lo B, Parham L. 2009. Ethical issues in stem cell research. Endocr Rev 30:204-13.

179. Lancaster MA, Renner M, Martin CA, Wenzel D, Bicknell LS, Hurles ME, Homfray T, Penninger JM, Jackson AP, Knoblich JA. 2013. Cerebral organoids model human brain development and microcephaly. Nature 501:373-9.

180. Elkabetz Y, Panagiotakos G, Al Shamy G, Socci ND, Tabar V, Studer L. 2008. Human ES cell-derived neural rosettes reveal a functionally distinct early neural stem cell stage. Genes Dev 22:152-65.

181. Gaspard N, Bouschet T, Hourez R, Dimidschstein J, Naeije G, van den Ameele J, Espuny-Camacho I, Herpoel A, Passante L, Schiffmann SN, Gaillard A, Vanderhaeghen P. 2008. An intrinsic mechanism of corticogenesis from embryonic stem cells. Nature 455:351-7.

182. Chambers SM, Fasano CA, Papapetrou EP, Tomishima M, Sadelain M, Studer L. 2009. Highly efficient neural conversion of human ES and iPS cells by dual inhibition of SMAD signaling. Nat Biotechnol 27:275-80.

183. Kadoshima T, Sakaguchi H, Nakano T, Soen M, Ando S, Eiraku M, Sasai Y. 2013. Self-organization of axial polarity, inside-out layer pattern, and species-specific progenitor dynamics in human ES cell-derived neocortex. Proc Natl Acad Sci U S A 110:20284-9.

184. Eiraku M, Watanabe K, Matsuo-Takasaki M, Kawada M, Yonemura S, Matsumura M, Wataya T, Nishiyama A, Muguruma K, Sasai Y. 2008. Self-organized formation of polarized cortical tissues from ESCs and its active manipulation by extrinsic signals. Cell Stem Cell 3:519-32.

185. Eiraku M, Takata N, Ishibashi H, Kawada M, Sakakura E, Okuda S, Sekiguchi K, Adachi T, Sasai Y. 2011. Self-organizing optic-cup morphogenesis in three-dimensional culture. Nature 472:51-6.

186. Nakano T, Ando S, Takata N, Kawada M, Muguruma K, Sekiguchi K, Saito K, Yonemura S, Eiraku M, Sasai Y. 2012. Self-formation of optic cups and storable stratified neural retina from human ESCs. Cell Stem Cell 10:771-785.

187. Chen HI, Song H, Ming GL. 2019. Applications of Human Brain Organoids to Clinical Problems. Dev Dyn 248:53-64.

188. Nasu M, Takata N, Danjo T, Sakaguchi H, Kadoshima T, Futaki S, Sekiguchi K, Eiraku M, Sasai Y. 2012. Robust formation and maintenance of continuous stratified cortical neuroepithelium by laminin-containing matrix in mouse ES cell culture. PLoS One 7:e53024.

189. Mariani J, Simonini MV, Palejev D, Tomasini L, Coppola G, Szekely AM, Horvath TL, Vaccarino FM. 2012. Modeling human cortical development in vitro using induced pluripotent stem cells. Proc Natl Acad Sci U S A 109:12770-5.

190. Qian X, Nguyen HN, Song MM, Hadiono C, Ogden SC, Hammack C, Yao B, Hamersky GR, Jacob F, Zhong C, Yoon KJ, Jeang W, Lin L, Li Y, Thakor J, Berg DA, Zhang C, Kang E, Chickering M, Nauen D, Ho CY, Wen Z, Christian KM, Shi PY, Maher BJ, Wu H, Jin P, Tang H, Song H, Ming GL. 2016. Brain-Region-Specific Organoids Using Mini-bioreactors for Modeling ZIKV Exposure. Cell 165:1238-1254.

191. Kelava I, Lancaster MA. 2016. Dishing out mini-brains: Current progress and future prospects in brain organoid research. Dev Biol 420:199-209.

192. Quadrato G, Nguyen T, Macosko EZ, Sherwood JL, Min Yang S, Berger DR, Maria N, Scholvin J, Goldman M, Kinney JP, Boyden ES, Lichtman JW, Williams ZM, McCarroll SA, Arlotta P. 2017. Cell diversity and network dynamics in photosensitive human brain organoids. Nature 545:48-53.

193. Watanabe M, Buth JE, Vishlaghi N, de la Torre-Ubieta L, Taxidis J, Khakh BS, Coppola G, Pearson CA, Yamauchi K, Gong D, Dai X, Damoiseaux R, Aliyari R, Liebscher S, Schenke-Layland K, Caneda C, Huang EJ, Zhang Y, Cheng G, Geschwind DH, Golshani P, Sun R, Novitch BG. 2017. Self-Organized Cerebral Organoids with Human-Specific Features Predict Effective Drugs to Combat Zika Virus Infection. Cell Rep 21:517-532.

194. Velasco S, Kedaigle AJ, Simmons SK, Nash A, Rocha M, Quadrato G, Paulsen B, Nguyen L, Adiconis X, Regev A, Levin JZ, Arlotta P. 2019. Individual brain organoids reproducibly form cell diversity of the human cerebral cortex. Nature 570:523-527.

195. Qian X, Song H, Ming GL. 2019. Brain organoids: advances, applications and challenges. Development 146.

196. Marton RM, Pasca SP. 2016. Neural Differentiation in the Third Dimension: Generating a Human Midbrain. Cell Stem Cell 19:145-146.

197. Monzel AS, Smits LM, Hemmer K, Hachi S, Moreno EL, van Wuellen T, Jarazo J, Walter J, Bruggemann I, Boussaad I, Berger E, Fleming RMT, Bolognin S, Schwamborn JC. 2017. Derivation of Human Midbrain-Specific Organoids from Neuroepithelial Stem Cells. Stem Cell Reports 8:1144-1154.

198. Jo J, Xiao Y, Sun AX, Cukuroglu E, Tran HD, Goke J, Tan ZY, Saw TY, Tan CP, Lokman H, Lee Y, Kim D, Ko HS, Kim SO, Park JH, Cho NJ, Hyde TM, Kleinman JE, Shin JH, Weinberger DR, Tan EK, Je HS, Ng HH. 2016. Midbrain-like Organoids from Human Pluripotent Stem Cells Contain Functional Dopaminergic and Neuromelanin-Producing Neurons. Cell Stem Cell 19:248-257.

199. Wataya T, Ando S, Muguruma K, Ikeda H, Watanabe K, Eiraku M, Kawada M, Takahashi J, Hashimoto N, Sasai Y. 2008. Minimization of exogenous signals in ES cell culture induces rostral hypothalamic differentiation. Proc Natl Acad Sci U S A 105:11796-801.

200. Muguruma K, Nishiyama A, Kawakami H, Hashimoto K, Sasai Y. 2015. Self-organization of polarized cerebellar tissue in 3D culture of human pluripotent stem cells. Cell Rep 10:537-50.

201. Ballabio C, Anderle M, Gianesello M, Lago C, Miele E, Cardano M, Aiello G, Piazza S, Caron D, Gianno F, Ciolfi A, Pedace L, Mastronuzzi A, Tartaglia M, Locatelli F, Ferretti E, Giangaspero F, Tiberi L. 2020. Modeling medulloblastoma in vivo and with human cerebellar organoids. Nat Commun 11:583.

202. Kasai T, Suga H, Sakakibara M, Ozone C, Matsumoto R, Kano M, Mitsumoto K, Ogawa K, Kodani Y, Nagasaki H, Inoshita N, Sugiyama M, Onoue T, Tsunekawa T, Ito Y, Takagi H, Hagiwara D, Iwama S, Goto M, Banno R, Takahashi J, Arima H. 2020. Hypothalamic Contribution to Pituitary Functions Is Recapitulated In Vitro Using 3D-Cultured Human iPS Cells. Cell Rep 30:18-24 e5.

203. Ozone C, Suga H, Eiraku M, Kadoshima T, Yonemura S, Takata N, Oiso Y, Tsuji T, Sasai Y. 2016. Functional anterior pituitary generated in self-organizing culture of human embryonic stem cells. Nat Commun 7:10351.

204. Suga H, Kadoshima T, Minaguchi M, Ohgushi M, Soen M, Nakano T, Takata N, Wataya T, Muguruma K, Miyoshi H, Yonemura S, Oiso Y, Sasai Y. 2011. Self-formation of functional adenohypophysis in three-dimensional culture. Nature 480:57-62.

205. Lukovic D, Artero Castro A, Kaya KD, Munezero D, Gieser L, Davo-Martinez C, Corton M, Cuenca N, Swaroop A, Ramamurthy V, Ayuso C, Erceg S. 2020. Retinal Organoids derived from hiPSCs of an AIPL1-LCA Patient Maintain Cytoarchitecture despite Reduced levels of Mutant AIPL1. Sci Rep 10:5426.

206. Zheng C, Schneider JW, Hsieh J. 2020. Role of RB1 in human embryonic stem cell-derived retinal organoids. Dev Biol doi:10.1016/j.ydbio.2020.03.011.

207. Wang Z, Wang SN, Xu TY, Miao ZW, Su DF, Miao CY. 2017. Organoid technology for brain and therapeutics research. CNS Neurosci Ther 23:771-778.

208. Terahara K, Yamamoto T, Mitsuki YY, Shibusawa K, Ishige M, Mizukoshi F, Kobayashi K, Tsunetsugu-Yokota Y. 2011. Fluorescent Reporter Signals, EGFP, and DsRed, Encoded in HIV-1 Facilitate the Detection of Productively Infected Cells and Cell-Associated Viral Replication Levels. Front Microbiol 2:280.

209. Fang A, Li D, Hao Z, Wang L, Pan B, Gao L, Qu X, He J. 2019. Effects of astrocyte on neuronal outgrowth in a layered 3D structure. Biomed Eng Online 18:74.

210. Gebert LF, Rebhan MA, Crivelli SE, Denzler R, Stoffel M, Hall J. 2014. Miravirsen (SPC3649) can inhibit the biogenesis of miR-122. Nucleic Acids Res 42:609-21.

211. Dello Russo C, Cappoli N, Coletta I, Mezzogori D, Paciello F, Pozzoli G, Navarra P, Battaglia A. 2018. The human microglial HMC3 cell line: where do we stand? A systematic literature review. J Neuroinflammation 15:259.

212. Li H, Zhang X, Chen M, Chen J, Gao T, Yao S. 2018. Dexmedetomidine inhibits inflammation in microglia cells under stimulation of LPS and ATP by c-Fos/NLRP3/caspase-1 cascades. EXCLI J 17:302-311.

213. Whitney JB, Hill AL, Sanisetty S, Penaloza-MacMaster P, Liu J, Shetty M, Parenteau L, Cabral C, Shields J, Blackmore S, Smith JY, Brinkman AL, Peter LE, Mathew SI, Smith KM, Borducchi EN, Rosenbloom DI, Lewis MG, Hattersley J, Li B, Hesselgesser J, Geleziunas R, Robb ML, Kim JH, Michael NL, Barouch DH. 2014. Rapid seeding of the viral reservoir prior to SIV viraemia in rhesus monkeys. Nature 512:74-7.

214. Dudani AK, Gupta RS, Gupta R. 1988. Species-specific differences in the toxicity of puromycin towards cultured human and Chinese hamster cells. FEBS Lett 234:141-4.

215. Man SM, Karki R, Kanneganti TD. 2017. Molecular mechanisms and functions of pyroptosis, inflammatory caspases and inflammasomes in infectious diseases. Immunol Rev 277:61-75.

216. Guarda G, Braun M, Staehli F, Tardivel A, Mattmann C, Forster I, Farlik M, Decker T, Du Pasquier RA, Romero P, Tschopp J. 2011. Type I interferon inhibits interleukin-1 production and inflammasome activation. Immunity 34:213-23.

217. Gao GF, Willcox BE, Wyer JR, Boulter JM, O'Callaghan CA, Maenaka K, Stuart DI, Jones EY, Van Der Merwe PA, Bell JI, Jakobsen BK. 2000. Classical and nonclassical class I major histocompatibility complex molecules exhibit subtle conformational differences that affect binding to CD8alphaalpha. J Biol Chem 275:15232-8.

218. Davis HR, Jr., Zhu LJ, Hoos LM, Tetzloff G, Maguire M, Liu J, Yao X, Iyer SP, Lam MH, Lund EG, Detmers PA, Graziano MP, Altmann SW. 2004. Niemann-Pick C1 Like 1 (NPC1L1) is the intestinal phytosterol and cholesterol transporter and a key modulator of whole-body cholesterol homeostasis. J Biol Chem 279:33586-92.

219. Graham DR, Chertova E, Hilburn JM, Arthur LO, Hildreth JE. 2003. Cholesterol depletion of human immunodeficiency virus type 1 and simian immunodeficiency virus with beta-cyclodextrin inactivates and permeabilizes the virions: evidence for virion-associated lipid rafts. J Virol 77:8237-48.

220. Nguyen DH, Hildreth JE. 2000. Evidence for budding of human immunodeficiency virus type 1 selectively from glycolipid-enriched membrane lipid rafts. J Virol 74:3264-72.

221. Zheng YH, Plemenitas A, Fielding CJ, Peterlin BM. 2003. Nef increases the synthesis of and transports cholesterol to lipid rafts and HIV-1 progeny virions. Proc Natl Acad Sci U S A 100:8460-5.

222. Sainz B, Jr., Barretto N, Martin DN, Hiraga N, Imamura M, Hussain S, Marsh KA, Yu X, Chayama K, Alrefai WA, Uprichard SL. 2012. Identification of the Niemann-Pick C1-like 1 cholesterol absorption receptor as a new hepatitis C virus entry factor. Nat Med 18:281-5.

223. Temel RE, Tang W, Ma Y, Rudel LL, Willingham MC, Ioannou YA, Davies JP, Nilsson LM, Yu L. 2007. Hepatic Niemann-Pick C1-like 1 regulates biliary cholesterol concentration and is a target of ezetimibe. J Clin Invest 117:1968-78.

224. Davis HR, Veltri EP. 2007. Zetia: inhibition of Niemann-Pick C1 Like 1 (NPC1L1) to reduce intestinal cholesterol absorption and treat hyperlipidemia. J Atheroscler Thromb 14:99-108.